J. Math. Biol. (1990) 28: 609–643

Journal of
Mathematical
Biology

A size dependent predator-prey interaction: who pursues whom?

A. M. De Roos[1], J. A. J. Metz[2], E. Evers[2], and A. Leipoldt[2]

[1] Department of Biological Sciences, University of Calgary, Calgary, Alberta T2N 1N4, Canada
[2] Institute of Theoretical Biology, Leiden University, Kaiserstraat 63, 2311 GP Leiden, The Netherlands

Received July 13, 1989; received in revised form January 3, 1990

Abstract. We investigate the properties of an (age, size)-structured model for a population of *Daphnia* that feeds on a dynamical algal food source. The stability of the internal equilibrium is studied in detail and combined with numerical studies on the dynamics of the model to obtain insight in the relation between individual behaviour and population dynamical phenomena. Particularly the change in the (age, size)-relation with a change in the food availability seems to be an important behavioural mechanism that strongly influences the dynamics. This influence is partly stabilizing and partly destabilizing and leads to the coexistence of a stable equilibrium and a stable limit cycle or even coexistence of two stable limit cycles for the same parameter values. The oscillations in this case are characterized by drastic changes in the size-structure of the population during a cycle. In addition the model exhibits the usual predator-prey oscillations that characterize Lotka–Volterra models.

Key words: Predator-prey interaction – Size-structured population dynamics – Behavioural mechanisms – Dynamical phenomena

1. Introduction

Especially in many ectothermic animal species the body size of an individual has a strong influence upon dynamical processes like its feeding, growth and reproduction [15, 18], which in turn affect the dynamics of the population as a whole. When we study the dynamics of and the interactions between populations within an ecosystem, we therefore cannot in general neglect the internal characteristics of these populations. In recent years the notion that the individual should be treated as the basic element in studying ecological systems has led to the development of various types of models that describe the dynamics of the total population in terms of the processes taking place at the level of the individual. In these models the behaviour of the individuals is allowed to differ due to differences in their physiological characteristics [5, 9] or differences in their spatial location [5, 17]. For example, if we want to take seriously the observation that body size is very important in determining individual behaviour ("behaviour" is used here in a population dynamical sense, i.e., to indicate feeding, growth, reproduction, etc.), we can turn to the class of "physiologically

structured population models" [9]. In these models the behaviour of an individual is assumed to depend on a limited set of its physiological characteristics only. The gain in biological realism, is, however, unavoidably coupled to an increased model complexity.

In classical, Lotka–Volterra type models of predator-prey interactions all prey individuals are lumped together, as well as all predator individuals, on the assumption that the interaction between the two populations can be completely described in terms of their total sizes. These models comprise only a limited number of mechanistic components: a component describing the autonomous growth in numbers of the prey and components describing the functional response, the numerical response and the death rate of the predator, respectively. The range of dynamics exhibited by the two populations is also limited: the sizes of the two populations either converge to a stable equilibrium or exhibit a specific type of oscillations, which will be more accurately described in a later section (in the biological literature the mechanism underlying the swtich from a stable equilibrium to a stable limit cycle is usually referred to as "the paradox of enrichment" [14]). Below we will refer to this type of models as unstructured ones, since the internal structure of both populations is neglected.

Incorporating more of the individual biology into a population dynamical model considerably increases the number of mechanistic components of the model. On the one hand the increased number of components may allow accounting for a much larger range of population dynamical phenomena. On the other hand it will become more and more difficult to assign any particular observed phenomenon to the action of particular mechanistic components. In-depth investigations into the relation between the mechanistic components of a physiologically structured population model and the dynamics exhibited by the total population are very rare. The recent development of an appropriate numerical method that is especially suited for physiologically structured population models makes studies of this type more feasible [3, 4]. In this paper we explore this field of investigation by studying the properties of a model for the dynamics of an (age, size)-structured predator population in interaction with its prey. For the prey population we assume that all individuals are essentially identical and therefore can be lumped together. Hence the prey population is only represented by its total size. We study the existence and stability properties of possible equilibria and try to unravel the mechanisms determining the stability. Numerical simulations of the dynamics of the two populations reveal characteristic dynamical phenomena which can be related to mechanistic components of the model. A wider range of dynamics than in the unstructured predator-prey models is observed, even to the extent that in some simulations the prey population seems to pursue the predator instead of vice versa.

2. The model of the individual behaviour

The model that we used for the population dynamical behaviour of an individual was introduced by Kooijman and Metz [7]. The Kooijman–Metz model was developed to describe the feeding, growth and reproduction of an individual *Daphnia magna* (waterflea) under various food conditions. Daphnids are filter feeders, using an assemblage of algae as their food source in a fairly indiscriminate way. Kooijman and Metz [7] used data on *Daphnia magna* feeding on *Chlorella* sp. to estimate the parameters of the model. The interaction between *Daphnia* and its algal food represents a more general class of biological systems in which a size-structured

predator population interacts with an unstructured population of prey. Although we will continuously refer to our populations as *Daphnia* and algae we will stress the properties and characteristics of the model that possibly generalize to the much wider class of predator-prey interactions. In the following we derive the model equations from the basic assumptions. For an experimental underpinning of these assumptions we refer to Kooijman and Metz [7].

Individual *Daphnia* of different sizes are assumed to have similar geometries, so that surface area and (wet) weight are proportional to the square and the cube of the individual length, respectively. In the following l will denote the size (length) of an individual, while a will denote its age. Instead of the surface area and (wet) weight of an individual we will just use l^2 and l^3, respectively. This will only affect some proportionality constants in the model. The concentration of algae, which can be taken as a measure of the food availability of the *Daphnia*, will be denoted by x. Table 1 summarizes the symbols used in the model to denote the various variables and parameters, the latter with their default value for *Daphnia magna* as inferred from [7].

The energy channelling within an individual *Daphnia* is schematically depicted in Fig. 1. The ingestion rate of algal cells by an individual is assumed to be proportional to its surface area, as is plausible for a filter-feeder. In addition this food intake rate,

Table 1. Symbol reference list for the variables and parameters used in the Kooijman–Metz model. The default parameters are extracted from [7]

Symbol	Default value	Description	Units
Variables			
a		Age	d(ays)
l		Length	mm
x		Concentration of edible algae	cell · ml^{-1}
Parameters			
l_b	0.8	Length at birth	mm
l_j	2.5	Length at maturation	mm
l_m	6.0	Maximum attainable length under infinite food availability	mm
γ	0.15	Time constant of growth	d^{-1}
ξ	7.0×10^{-6}	Shape parameter of the functional response	ml · cell^{-1}
v_x	1.8×10^6	Maximum feeding rate per unit surface area	cell · mm^{-2} · d^{-1}
κ	0.3	Default fraction of ingested energy channelled to growth and maintenance	—
r_m	0.1	Maximum reproduction rate per unit surface area	mm^{-2} · d^{-1}
μ	variable	Random death rate of *Daphnia*	d^{-1}
$A_{\max}$	70	Maximum lifetime of *Daphnia*	d
$X_{\max}$	variable	Maximum concentration of algae in the absence of *Daphnia*	cell · ml^{-1}
α	0.5	Flow-through rate in case of chemostat algal dynamics	d^{-1}
β	0.5	Maximum algal growth rate in case of logistic algal growth	d^{-1}

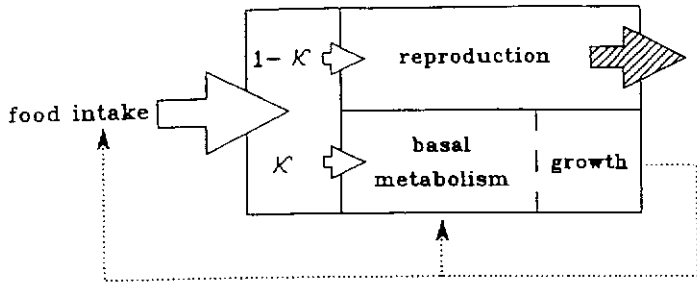

Fig. 1. A schematic representation of the energy channelling in the *Daphnia* model

denoted by $I(x, l)$, at any given individual size depends on the prevailing algal density following a Holling type II functional response. Hence,

$$I(x, l) = v_x f(x) l^2, \qquad f(x) = \frac{\xi x}{1 + \xi x}, \tag{1}$$

where v_x is the product of the maximum intake rate of algal cells per unit surface area and the proportionality constant relating surface area to l^2. The function $f(x)$ equals a Holling type II functional response scaled between 0 and 1. ξ is the shape parameter of the functional response. Equation (1) can equivalently be expressed in terms of the amount of energy assimilated per unit time, by replacing v_x with its analogue v_e: the product of the maximum energy assimilation rate times the proportionality constant relating surface area to l^2. The quotient v_e/v_x then determines the conversion of ingested algal cells to assimilated energy, i.e., v_e/v_x is the product of the energy content per algal cell and the assimilation efficiency, which is assumed to be constant.

Under conditions of sufficient food availability the ingested energy is allocated in fixed proportions κ and $1-\kappa$ to growth plus maintenance on the one hand and maturation plus reproduction on the other. Here, sufficient means that the default allotment of ingested energy to growth plus maintenance can at least cover maintenance requirements alone. These requirements are assumed to be proportional to an animal's wet weight and therefore to l^3, with proportionality constant ζ. Furthermore, growth in size only occurs when maintenance has had its share. The energy requirements for growth per unit weight increase are assumed to be constant. The product of these energy requirements and the proportionality factor relating weight to l^3 will be called η.

Individuals are assumed not to shrink in size. Therefore, in case the default allotment of ingested energy to growth plus maintenance is not sufficient to cover maintenance alone, energy rechannelling takes place. Ingested energy is then allocated in such a way that growth stops, maintenance requirements are just met and the remaining energy is channelled to maturation plus reproduction. The Kooijman–Metz model does not account for the presence of energy reserves within an individual. If the ingested energy is less than the maintenance requirements, the individual is assumed to die instantaneously (see below).

These assumptions lead to a slightly adapted von Bertalanffy growth equation [2] for the growth in weight under sufficient food conditions. If the weight of an individual is denoted by w, this growth equation can be expressed as

$$\frac{dw}{dt} = \begin{cases} \dfrac{1}{\eta}(\kappa v_e f(x) w^{2/3} - \zeta w) & \text{for } w < \dfrac{\kappa v_e}{\zeta} f(x) w^{2/3} \\ 0 & \text{otherwise.} \end{cases}$$

The proportionality assumptions now imply that $w = l^3$ and $w^{2/3} = l^2$. Substituting these equalities into the equation above yields the following equation describing the

growth in length:

$$\frac{dl}{dt} = g(x, l) = \begin{cases} \frac{1}{3\eta}(\kappa v_e f(x) - \zeta l) & \text{for } l < \frac{\kappa v_e}{\zeta} f(x) \\ 0 & \text{otherwise.} \end{cases}$$

Defining $l_m := \kappa v_e / \zeta$ as the maximum length that an individual can attain under unlimited food availability and $\gamma := \zeta / 3\eta$ as the rate constant of growth this equation can be rewritten as

$$\frac{dl}{dt} = g(x, l) = \begin{cases} \gamma(l_m f(x) - l) & \text{for } l < l_m f(x) \\ 0 & \text{otherwise.} \end{cases} \tag{2}$$

in which $l_m f(x)$ represents the maximum attainable length under the prevailing food conditions. This length $l_m f(x)$ equals the length at which growth just stops and the default allocation of energy to growth of maintenance can just cover maintenance completely. At time of birth all the individuals are assumed to have an identical size l_b.

A juvenile individual is assumed to become an adult on reaching a fixed length l_j. The energy channelled to maturation plus reproduction is assumed to be used solely for maturation while $l < l_j$ and solely for reproduction while $l \geqslant l_j$. The energy costs for producing one young we will call $1/\theta$. The reproduction rate $b(x, l)$ hence equals

$$b(x, l) = \begin{cases} 0 & \text{for } l_b \leqslant l < l_j \\ \theta(1 - \kappa) v_e f(x) l^2 & \text{for } l_j \leqslant l < \frac{\kappa v_e}{\zeta} f(x) \\ \theta(v_e f(x) l^2 - \zeta l^3) & \text{otherwise} \end{cases}$$

or, defining $r_m := \theta(1 - \kappa) v_e$ as the maximum reproduction rate per unit surface area times the proportionality constant relating surface area to l^2:

$$b(x, l) = \begin{cases} 0 & \text{for } l_b \leqslant l < l_j \\ r_m f(x) l^2 & \text{for } l_j \leqslant l < l_m f(x) \\ \frac{r_m}{(1 - \kappa)} \left(f(x) l^2 - \frac{\kappa l^3}{l_m} \right) & \text{otherwise.} \end{cases} \tag{3}$$

The latter parts of these formulae express that for $l > l_m f(x)$ the reproduction rate changes due to the rechannelling of ingested energy to cover maintenance. These formulae indicate that in principle $b(x, l)$ can drop below 0, due to this rechannelling of ingested energy. However, this will only occur if the ingested energy is not sufficient to cover the maintenance requirements. In this case the individual is assumed to die instantaneously, as mentioned above.

Individual *Daphnia* are assumed to die at random due to, for example, predation. Additional causes of death that are accounted for in the model are death from old age and death from starvation. Death from old age is incorporated into the model by assuming instant death on reaching the maximum lifetime $A_{\max}$. Death from starvation means that an individual dies instantaneously when it cannot cover its maintenance requirements anymore. The individual death rate can therefore be expressed as

$$d(x, a, l) = \begin{cases} \mu & \text{for } a < A_{\max} \text{ and } l < \frac{l_m f(x)}{\kappa} \\ \infty & \text{otherwise,} \end{cases} \tag{4}$$

in which μ is the random death rate and $l_m f(x)/\kappa$ is the length at which maintenance requirements just equal the amount of energy ingested.

Since we will not discriminate between individual algal cells, we will treat the concentration of edible algae as one dynamically varying quantity. Therefore, in the following the phrases "population" and "individuals" will be exclusively used for the *Daphnia* (or predator, in general), unless explicitly stated otherwise. The population of edible algae (or prey population in general) will frequently be referred to as "food availability".

For the autonomous rate of change of the algae in the absence of *Daphnia*, denoted by $R(x)$, we will choose

$$R(x) = \alpha(X_{\max} - x) \tag{5a}$$

or:

$$R(x) = \beta x\left(1 - \frac{x}{X_{\max}}\right) \tag{5b}$$

Equation (5a) represents a chemostat type dynamics of the algae, in which $X_{\max}$ is the algal concentration in the input and α is the relative flow-through rate. This type of dynamics reflects an experimental situation in which a *Daphnia* population is continuously fed with an algal suspension of constant density. Equation (5b) represents a logistic type of dynamics, in which β is the maximum rate of increase and $X_{\max}$ the carrying capacity of the algal population. This latter type of dynamics reflects a more natural population growth process. In both cases $X_{\max}$ is the maximum algal density that can be reached in the absence of *Daphnia*. It is obvious that $R(x) > 0$ for $0 < x < X_{\max}$.

3. The model for the population dynamics

As the individual *Daphnia* can attain ages within $[0; A_{\max})$ and lengths within $[l_b; l_m)$, the biological population can be represented by a density function $n(t, a, l)$ over $\Omega := [0, A_{\max}) \times [l_b; l_m)$: the rectangle spanned by the attainable age- and size-ranges. The quantity

$$\int_{l_1}^{l_2}\int_{a_1}^{a_2} n(t, a, l)\, da\, dl$$

then represents the number of individuals with an age between a_1 and a_2 and an individual size between l_1 and l_2. On the basis of the modelled individual behaviour from the previous section a set of equations for the density function $n(t, a, l)$ can be formulated, which describe the dynamics of the total population. Following the lines set out by Metz and Diekmann ([9], see also [10]) we arrive at

$$\frac{\partial n}{\partial t} + \frac{\partial n}{\partial a} + \frac{\partial gn}{\partial l} = -dn, \tag{6a}$$

$$n(t, 0, l) = \delta(l - l_b)\int_{\Omega} b(x, l)n(t, a, l)\, da\, dl, \tag{6b}$$

$$n(0, a, l) = \Psi(a, l). \tag{6c}$$

In these equations (and in all the following) we have refrained from writing the arguments of any function in full if the context makes clear what these arguments are. The functions g, b and d are the individual behaviour functions given in formulae

(2)–(4). The "function" δ denotes the Dirac delta function and $\Psi(a, l)$ represents the inital (age, size)-distribution, which is assumed to be known. The hyperbolic partial differential equation (PDE) (6a) describes the growth, ageing and dying of the individuals in the population, while the side condition (6b) represents the reproduction of all the individuals. The appearance of the Dirac delta function $\delta(l - l_b)$ results from the assumption that all individuals are born with the same size l_b. Since we assume that all individuals in the population experience the same environmental conditions and the growth of an individual is deterministic, the "equal size at birth" assumption causes all individuals that are born at one particular time to stay together as a cohort (= a group of identical individuals) during their entire life. This leads to a degeneracy of the density function n. Although the initial (age, size)-distribution can have the whole state-space Ω as its support, the density function n will ultimately settle down on an only one-dimensional support in Ω, representing the current (age, size)-relation. On the one hand the "equal size at birth" assumption thus makes the system (6) slightly unpleasant, *inter alia*, for the calculation of equilibria. On the other hand, however, particularly this assumption ensures that we can derive a characteristic equation to study the stability properties of the equilibria, as is noted in [10].

For the calculation of the equilibria and the analysis of their stability we will reformulate the system of Eqs. (6). The "equal size at birth" assumption implies that a every time t there exists a unique relation between the size and the age of the individual (at least after the initial population has died out). This (age, size)-relation, which will be denoted by $l(t, a)$, essentially specifies at every time t the characteristic of the PDE (6a), i.e., the one-dimensional support of the density function n in Ω.

The original set of equations can now be rewritten using a technique that has been called the "Murphy trick" [9, 11]. Here we will only briefly outline this technique. Instead of a representation by means of one density function $n(t, a, l)$, the *Daphnia* population is equivalently characterized by the current (age, size)-relation $l(t, a)$ in combination with a separate density function $m(t, a)$, which describes the age-distribution of the *Daphnia* population. The equations for the dynamics of $m(t, a)$ and $l(t, a)$ can be derived by following one cohort of identical individuals through time, i.e., by focussing on the value and dynamics of $m(t, a)$ and $l(t, a)$ at a fixed time t and a fixed age a. Essentially this means that the model is reformulated in terms of the derivatives along the characteristics of the original PDE (6a).

Let τ denote a variable equivalent with time except for an arbitrariness of its origin. If we follow one cohort of identical individuals, we can intuitively write down that

$$\frac{dl}{d\tau} = \frac{\partial l}{\partial t} + \frac{\partial l}{\partial a} = g(x, l(t, a))$$

and

$$\frac{dm}{d\tau} = \frac{\partial m}{\partial t} + \frac{\partial m}{\partial a} = -d(x, a, l(t, a))m(t, a),$$

which eventually leads to the reformulated set of equations:

$$\frac{\partial m}{\partial t} + \frac{\partial m}{\partial a} = -d(x, a, l(t, a))m(t, a), \tag{7a}$$

$$m(t, 0) = \int_0^{A_{\max}} b(x, l(t, a))m(t, a)\, da, \tag{7b}$$

$$\frac{\partial l}{\partial t} + \frac{\partial l}{\partial a} = g(x, l(t, a)), \tag{7c}$$

$$l(t, 0) = l_b, \tag{7d}$$

$$m(0, a) = \Phi(a), \qquad l(0, a) = \Gamma(a) \tag{7e}$$

provided the initial state of the population is such that a well-defined (age, size)-relation $\Gamma(a)$ exists at $t = 0$. The PDE (7a) describes the evolution of the age-distribution $m(t, a)$ in time, while the side condition (7b) again represents the reproduction process. Equations (7c) and (7d) describe the evolution of the current (age, size)-relation in the population. The initial condition consists of two functions: $\Phi(a)$ and $\Gamma(a)$, which describe the initial age-distribution and the initial (age, size)-relation, respectively.

Since the food availability is a dynamically varying quantity we have to add the following equation for the food dynamics to the system (7):

$$\frac{dx}{dt} = R(x) - \int_0^{A_{\max}} I(x, l(t, a))m(t, a)\, da, \qquad x(0) = x_0 \tag{8}$$

in which $R(x)$ describes the autonomous dynamics of the algal population as given by Eq. (5a) or (5b) and $I(x, l)$ is the food intake rate given by Eq. (1).

Together the system of Eqs. (7) and (8) specify the model of the predator-prey interaction under consideration. In the following sections we will focus upon the existence and stability of internal equilibria and the possible types of dynamics in the model. We will pay no attention to the trivial equilibrium ($x = X_{\max}$, $m(t, a) = 0$) in which the algal population is at its maximum density and the *Daphnia* are absent.

4. Equilibria

First we will introduce some notation: the food availability at equilibrium will be denoted by $\tilde{x}$. The age-distribution and the (age, size)-relation of the *Daphnia* population at equilibrium will similarly be denoted by $\tilde{m}(a)$ and $\tilde{l}(a)$, respectively.

The growth of an individual *Daphnia* is described by Eq. (2) as a function of its size and and the current food availability. If the food level x is constant in time, this equation can be solved, yielding

$$l^*(a, x) = l_m f(x) - (l_m f(x) - l_b)\, e^{-\gamma a}. \tag{9a}$$

Here we have used the notation $l^*(a, x)$ to denote the size of an individual with age a, that has been living at the *constant* food level x. Equation (9a) represents a von Bertalanffy growth curve.

The equilibrium (age, size)-relation within the *Daphnia* population can be obtained from (7c), assuming $\partial l/\partial t = 0$ and solving the resulting equation. Necessarily, however, the equilibrium (age, size)-relation is of the form (9a) and we can therefore write

$$\tilde{l}(a) = l^*(a, \tilde{x}). \tag{9b}$$

Equations (9) also make clear that death by starvation does not occur in equilibrium situations, because $\tilde{l}(a) < l_m f(\tilde{x})$ for all a. In equilibrium Eq. (4) hence becomes

$$d(\tilde{x}, a, \tilde{l}(a)) = \begin{cases} \mu & \text{for } a < A_{\max} \\ \infty & \text{for } a \geqslant A_{\max}. \end{cases}$$

The age-distribution in equilibrium, $\tilde{m}(a)$, can now be derived by putting $\partial m/\partial t = 0$ in (7a), substituting the above expression for $d(\tilde{x}, a, \tilde{l}(a))$ and solving the resulting

equation. This yields

$$\tilde{m}(a) = \begin{cases} \tilde{m}(0)F(a) & \text{for } a < A_{\max} \\ 0 & \text{for } a \geqslant A_{\max} \end{cases} \tag{10}$$

with $F(a) = \exp(-\mu a)$ the survival function up to age a of an individual *Daphnia*.

Since $\tilde{l}(a) < l_m f(\tilde{x})$, Eq. (3) simplifies in equilibrium to

$$b(\tilde{x}, \tilde{l}(a)) = \begin{cases} 0 & \text{for } l_b \leqslant \tilde{l}(a) < l_j \\ r_m f(\tilde{x})[\tilde{l}(a)]^2 & \text{for } \tilde{l}(a) \geqslant l_j. \end{cases}$$

The age at which reproduction starts can be derived from solving the set of Eqs. (9) for $\tilde{l}(a) = l_j$. This age value will be called the age at maturation and will be denoted by A_j. Obviously, A_j depends on the food availability $\tilde{x}$. Substituting the expression above for $b(\tilde{x}, \tilde{l}(a))$ and the expressions (9) and (10) for $\tilde{l}(a)$ and $\tilde{m}(a)$, respectively, into the side condition (7b) yields the following, implicit equilibrium equation:

$$P(\tilde{x}) = 1 \tag{11a}$$

with

$$P(x) = \int_{A_j(x)}^{A_{\max}} b(x, l^*(a, x))F(a)\,da = \int_{A_j(x)}^{A_{\max}} r_m f(x)[l^*(a, x)]^2 F(a)\,da \tag{11b}$$

and

$$A_j(x) = \frac{1}{\gamma} \ln\left(\frac{l_m f(x) - l_b}{l_m f(x) - l_j}\right). \tag{11c}$$

As mentioned before, $A_j(x)$ represents the age at maturation under the constant food availability x, i.e., $l^*(A_j(x), x) = l_j$. The function $P(x)$ can be interpreted as the expected number of offspring that an individual *Daphnia* becomes during its entire lifetime, when experiencing a constant food availability x. In equilibrium ($x = \tilde{x}$) this should clearly equal 1.

The unknown variable, for which the system of Eqs. (11) has to be solved, is the food density $\tilde{x}$ (or equivalently the quantity $f(\tilde{x})$, the value of the functional response at $\tilde{x}$). This result shows that the food level at equilibrium is determined completely by the characteristics of the *Daphnia* population. As a consequence also the internal structure of the *Daphnia* population at equilibrium is completely set by the parameters of the functions (1)–(4), describing the individual behaviour. Only the absolute density of *Daphnia* at equilibrium is derived from Eq. (8) for the algal dynamics:

$$\begin{aligned} 0 = \frac{d\tilde{x}}{dt} &= R(\tilde{x}) - \int_0^{A_{\max}} I(\tilde{x}, \tilde{l}(a))\tilde{m}(a)\,da \\ &= R(\tilde{x}) - \int_0^{A_{\max}} v_x f(\tilde{x})[\tilde{l}(a)]^2 \tilde{m}(0)F(a)\,da, \end{aligned} \tag{12}$$

which explicitly yields $\tilde{m}(0)$ as a function of $\tilde{x}$ and hence determines the total population size.

The function $P(x)$ defined in (11b) has the following properties:

$$P(x_c) = 0, \tag{13a}$$

$$\frac{\partial P}{\partial x} > 0, \qquad \text{for } x > x_c, \tag{13b}$$

in which x_c is the unique solution of $A_j(x) = A_{\max}$. This food level x_c represents the food level, below which an individual *Daphnia* would never reach adulthood during

its entire lifetime. Hence for $x < x_c$ a *Daphnia* population can never survive and no equilibrium can exist. The property (13b) also follows intuitively from the biological interpretation of the function $P(x)$.

Equations (11) and (12) hence specify a unique, internal equilibrium $(\tilde{x}, \tilde{m}(a), \tilde{l}(a))$, if and only if $P(X_{\max}) > 1$. These conditions imply that the *minimum* value of $X_{\max}$ (given by $P(X_{\max}) = 1$), for which an internal equilibrium can just exist, exactly equals the food availability $\tilde{x}$ at equilibrium. In other words, in equilibrium the *Daphnia* population exploits its food source to the utmost. The equilibrium food availability $\tilde{x}$ is an increasing function of the death rate μ of the *Daphnia*, as can be inferred from Eq. (11b) by taking the derivative of $P(x)$ with respect to μ. Moreover, the equilibrium *Daphnia* density $\tilde{m}(a)$ is at every age value an increasing function of $R(\tilde{x})$ and hence also of $X_{\max}$.

5. The stability analysis

The main purpose of this paper is to establish relations between behavioural mechanisms on the level of the individual and dynamical phenomena on the level of the population. We will therefore study in detail the stability of the internal equilibrium from the previous section and combine the insights obtained from this stability analysis with the results obtained from numerical simulations of the dynamics of the model.

The stability analysis of the internal equilibrium is not a straightforward procedure. At present the existing general theory on structured population models of the type that we study in this paper is not yet sufficiently developed to answer even the first questions about the existence and uniqueness of solutions and the validity of the linearized stability principle. In principle this means that at present there exists no valid and mathematically rigorous technique to analyze the stability of the internal equilibrium. Moreover, Thieme [16] has shown that with very specific initial conditions the Kooijman–Metz model as specified by (7) and (8) does not guarantee the uniqueness of a solution, i.e., the model that we are studying is essentially not well posed. Fortunately, these specific conditions are such that from a biological point of view we can safely ignore this complication.

The lack of rigorous mathematical theory and theorems that are formally necessary to study the stability of the internal equilibrium left us only one route to follow: relying on the analogy with the existing theory on dynamical systems we straightforwardly linearized the model equations around the internal equilibrium state and substituted trial solutions of the form $c \cdot \exp(\lambda t)$. As a result we were able to derive a characteristic equation in the single variable λ. The roots of this characteristic equation determine the stability of the equilibrium. The results of this procedure were continuously checked and compared with numerical simulations of the dynamics of the model like we present in a later section. The fact that the results from these two routes of investigation matched, inspires some trust in both the validity of the performed stability analysis and the correctness of the numerical scheme.

As was shown in the previous section an internal equilibrium exists if $P(X_{\max}) > 1$. (Note that $P(X_{\max}) > 1$ also implies $X_{\max} > x_c$.) Moreover, the equilibrium food availability $\tilde{x}$ is completely determined by the parameters l_b, l_j, l_m, γ, r_m, μ and $A_{\max}$ that occur in the functions (1)–(4) describing the *Daphnia* individual behaviour. Hence, using $X_{\max}$ as a bifurcation parameter we can deduce that the branch of internal equilibria bifurcates from the trivial equilibrium $(X_{\max}, 0)$ at $X_{\max} = \tilde{x}$. The general results from bifurcation theory then suggest that at least for $X_{\max}$ slightly

larger than $\tilde{x}$ the internal equilibrium is stable. The uniqueness of the internal equilibrium subsequently implies that a destabilization of the equilibrium can only occur if a conjugate pair of complex eigenvalues passes the imaginary axis from left to right, presumably coinciding with a Hopf bifurcation. From this a stable or unstable limit cycle arises.

Deriving a characteristic equation in the single complex variable λ was only possible because all individual *Daphnia* are born with the equal size l_b [10] and was greatly facilitated by rewriting the original system of Eqs. (6) into the system (7). In the appendix the derivation of the characteristic equation by linearization of (7) and (8) and substitution of trial solutions of the form $c \cdot \exp(\lambda t)$ will be outlined in more detail. Here we will only give the final equation as we intend to study the stabilizing and destabilizing components in it.

In the following we will write $\tilde{b}$ instead of $\tilde{m}(0)$ to denote the birth rate of the total *Daphnia* population in equilibrium. We also introduce the functions

$$\bar{A}_r(s) = \tilde{b} \int_{A_j(\tilde{x})}^{A_{\max}} e^{-sa} r_m f(\tilde{x}) [\tilde{l}(a)]^2 F(a)\, da, \tag{14a}$$

$$\bar{A}_f(s) = \tilde{b} \int_0^{A_{\max}} e^{-sa} v_x f(\tilde{x}) [\tilde{l}(a)]^2 F(a)\, da. \tag{14b}$$

$\bar{A}_r(s)$ and $\bar{A}_f(s)$ are the Laplace transforms of the density functions that describe the reproduction rate and the food intake rate, respectively, for the total *Daphnia* population in equilibrium. Using this notation, the equilibrium equations (11) and (12) can be written as

$$\bar{A}_r(0) = \tilde{b}, \tag{15a}$$

$$\bar{A}_f(0) = R(\tilde{x}). \tag{15b}$$

After linearization and substitution of exponential trial solutions (see the appendix) a system of equations results of the form:

$$S(\lambda) \cdot \Delta \overset{\text{def}}{=} \begin{pmatrix} s_{11} & s_{12} \\ s_{21} & s_{22} \end{pmatrix} \begin{pmatrix} \Delta_b \\ \Delta_x \end{pmatrix}, \tag{16}$$

in which Δ_b and Δ_x denote small deviations from the equilibrium values of the population birth rate $\tilde{b}$ and the food availability $\tilde{x}$, respectively. The stability matrix S only depends on λ and the equilibrium state values of the whole system. The eigenvalues of the system are now the roots of

$$\det S(\lambda) = 0. \tag{17a}$$

The elements of the matrix S are given by

$$s_{11} = \frac{\bar{A}_r(\lambda)}{\tilde{b}} - 1, \tag{17b}$$

$$s_{21} = -\frac{\bar{A}_f(\lambda)}{\tilde{b}}, \tag{17c}$$

$$s_{12} = \frac{\bar{A}_r(0) f'(\tilde{x})}{f(\tilde{x})} + \left\{ \frac{r_m f(\tilde{x}) l_m f(\tilde{x}) l_j^2}{(l_m f(\tilde{x}) - l_j)} \tilde{b} F(A_j(\tilde{x})) \frac{1 - e^{-(\lambda+\gamma) A_j(\tilde{x})}}{\lambda + \gamma} \right.$$

$$\left. + 2\gamma r_m f(\tilde{x}) l_m f(\tilde{x}) \int_{A_j(\tilde{x})}^{A_{\max}} \tilde{l}(a) \tilde{b} F(a) \frac{1 - e^{-(\lambda+\gamma)a}}{\lambda + \gamma}\, da \right\} \frac{f'(\tilde{x})}{f(\tilde{x})}, \tag{17d}$$

$$s_{22} = R'(\tilde{x}) - \lambda - \frac{\bar{A}_f(0) f'(\tilde{x})}{f(\tilde{x})} - \left\{ 2\gamma v_x f(\tilde{x}) l_m f(\tilde{x}) \int_0^{A_{\max}} \bar{l}(a) \bar{b} F(a) \frac{1 - e^{-(\lambda+\gamma)a}}{\lambda + \gamma} da \right\} \frac{f'(\tilde{x})}{f(\tilde{x})}, \tag{17e}$$

with $f'(x)$ and $R'(x)$ the derivatives of $f(x)$ and $R(x)$, respectively, to x.

In the next section we will consider the numerical exploration of the characteristic equation (17). It is, however, very informative to compare the stability matrix S with the stability matrix of an equivalent, unstructured predator-prey model for the interaction of the *Daphnia* population with its algal food source. Let in this context $x_u(t)$ denote the number of algae and $m_u(t)$ the number of *Daphnia* present at time t. An unstructured caricature of the population model that we study in this paper is

$$\frac{dm_u}{dt} = r_m l_u^2 f(x_u) m_u - \mu m_u, \tag{18a}$$

$$\frac{dx_u}{dt} = R(x_u) - v_x l_u^2 f(x_u) m_u, \tag{18b}$$

in which l_u now is a parameter that denotes the identical size characterizing all the individual *Daphnia*. The parameters v_x, r_m and μ and the functions $R(x_u)$ and $f(x_u)$ are the same as in the structured model. The food availability at equilibrium $\tilde{x}_u$ and *Daphnia* density at equilibrium $\tilde{m}_u$ in this unstructured model now satisfy

$$r_m l_u^2 f(\tilde{x}_u) = \mu, \tag{19a}$$

$$v_x l_u^2 f(\tilde{x}_u) \tilde{m}_u = R(\tilde{x}_u). \tag{19b}$$

The stability of this equilibrium is governed by the following characteristic equation, that results from straightforward linearization:

$$\det U(\lambda) \overset{\text{def}}{=} \det \begin{pmatrix} u_{11} & u_{12} \\ u_{21} & u_{22} \end{pmatrix} \overset{\text{def}}{=} \det \begin{pmatrix} -\lambda & r_m l_u^2 f'(\tilde{x}_u) \tilde{m}_u \\ -v_x l_u^2 f(\tilde{x}_u) & R'(\tilde{x}_u) - \lambda - v_x l_u^2 f'(\tilde{x}_u) \tilde{m}_u \end{pmatrix} = 0. \tag{20}$$

Applying the Routh–Hurwitz criterion [12] to the quadratic expression in λ that follows from Eq. (20) results in the single condition for stability:

$$v_x l_u^2 f'(\tilde{x}_u) \tilde{m}_u > R'(\tilde{x}_u). \tag{21}$$

Condition (21) can be interpreted in the following way: the equilibrium specified by (19) is stable if the food intake rate of the total predator population in equilibrium increases (decreases) faster than the growth rate of the prey population with an increase (decrease) in the prey density. Or conversely, instability of the equilibrium results only if the prey population can escape the control imposed by the feeding of the predator population. For this reason we will refer to this destabilizing mechanism as *prey escape mechanism*.

If we want to compare the stability matrices S and U (Eqs. (17) and (20)) we first have to identify some quantities from the size-structured predator-prey model with their unstructured equivalents: in the structured model the *Daphnia* population birth rate in equilibrium was denoted by $\bar{b}$ and was equal to $\bar{A}_r(0)$. We will denote the equivalent quantity in the unstructured model by $\bar{b}_u$, which now equals $r_m l_u^2 f(\tilde{x}_u) \tilde{m}_u$. In the same way the food intake rate of the *Daphnia* population, which was denoted

by $\bar{A}_f(0)$ in the structured model, can be related to the quantity $v_x l_u^2 f(\tilde{x}_u)\tilde{m}_u$ in the unstructured model.

An obvious difference between the structured and the unstructured model is the presence of a delay $A_j(x)$ in the structured model between the birth of an individual, at which time it also starts feeding, and the onset of reproduction by that specific individual. Generally speaking such a delay will have a destabilizing influence upon the equilibrium. Apart from this difference the first columns of the two matrices, although not identical, are at least comparable. To show this we notice that the equilibrium *Daphnia* population in the unstructured model can also be described by the density function $\tilde{b}_u F(a)$, in which $F(a) = \exp(-\mu a)$ represents the exponential survival function of the *Daphnia* (compare Eq. (10)) and $\tilde{b}_u$ is the population birth rate as defined above. The quantity $\tilde{m}_u$ that appears in the preceding Eqs. (19)–(21) is obviously related to this density function in the following way:

$$\tilde{m}_u = \int_0^\infty \tilde{b}_u F(a)\, da. \tag{22}$$

(Note that the substitution of $r_m l_u^2 f(\tilde{x}_u)\tilde{m}_u$ for $\tilde{b}_u$ in this equation would result in the first equilibrium equation as specified by (19a).)

Using this density function $\tilde{b}_u F(a)$ we can derive the functions $\bar{A}_{ru}(s)$ and $\bar{A}_{fu}(s)$ that are analogous with the functions $\bar{A}_r(s)$ and $\bar{A}_f(s)$, respectively, from the structured model (Eqs. (14a) and (14b)):

$$\bar{A}_{ru}(s) = \tilde{b}_u \int_0^{A_{\max}} e^{-sa} r_m l_u^2 f(\tilde{x}_u) F(a)\, da = \frac{r_m l_u^2 f(\tilde{x}_u)\tilde{b}_u}{s+\mu}, \tag{23a}$$

$$\bar{A}_{fu}(s) = \tilde{b}_u \int_0^{A_{\max}} e^{-sa} v_x l_u^2 f(\tilde{x}_u) F(a)\, da = \frac{v_x l_u^2 f(\tilde{x}_u)\tilde{b}_u}{s+\mu}. \tag{23b}$$

In accordance with the interpretations of the functions $\bar{A}_r(s)$ and $\bar{A}_f(s)$ in the structured model, the functions $\bar{A}_{ru}(s)$ and $\bar{A}_{fu}(s)$ from the unstructured model are the Laplace transforms of the density functions that describe the reproduction and the food intake rate, respectively, for the total *Daphnia* population in equilibrium. We can now write for u_{11} and u_{21}:

$$u_{11} = \left[\frac{\bar{A}_{ru}(\lambda)}{\tilde{b}_u} - 1\right](\lambda + \mu), \tag{24a}$$

$$u_{21} = -\frac{\bar{A}_{fu}(\lambda)}{\tilde{b}_u}(\lambda + \mu), \tag{24b}$$

from which we conclude that the first column of U is comparable with the first column of S, except for a scaling factor $(\lambda + \mu)$. This scaling factor is due to the fact that the linearization in the unstructured model was done in terms of the quantity $\tilde{m}_u$, the total *Daphnia* population size in equilibrium, as opposed to $\tilde{b}$, the population birth rate in equilibrium, used in the structured model. The scaling factor $(\lambda + \mu)$ will obviously occur in both terms of $\det U(\lambda)$ (see Eq. (20)) and its influence will hence be limited to the introduction of a root $\lambda = -\mu$ of the characteristic equation $\det U(\lambda) = 0$. Therefore, the factor will not influence the roots of the characteristic equation that determine the stability of the unstructured model.

The main differences between the two matrices S and U hence are the terms between braces in the elements s_{12} and s_{22}. These differences indicate the additional mechanisms present in the structured predator-prey model that can stabilize or destabilize the steady state and hence induce a wider range of dynamics. Apart from these terms within braces the second column of the matrix S is completely identical

with the second column of U, given the equivalences between $\bar{A}_r(0)$ and $r_m l_u^2 f(\tilde{x}_u)\tilde{m}_u$ and between $\bar{A}_f(0)$ and $v_x l_u^2 f(\tilde{x}_u)\tilde{m}_u$, mentioned before.

In both the structured and the unstructured model a slight deviation in the food availability at equilibrium will directly affect the reproduction and the food intake rate of the *Daphnia* population, as is reflected in the common terms in the second column of the matrices S and U. In the structured model, however, such a slight deviation also has indirect effects upon the reproduction and the food intake rate of the *Daphnia* via a change in the current (age, size)-relation within the population. These indirect effects are reflected by the terms within braces in (17d) and (17e). The effect upon the reproduction rate is even twofold, as is clear from the two terms within braces in s_{12} ((Eq. 17d)): a change in the food availability changes the current (age, size)-relation of the adults and thus the reproduction capacity of the individual *Daphnia*, but also changes the duration of the juvenile period. The food intake rate is only affected by the change in the (age, size)-relation, because this induces a change in the feeding capacity of the individuals. This interpretation of the origin of the braced terms in s_{12} and s_{22} is deduced from the derivation of the characteristic equation (see the appendix).

From the foregoing comparison between the stability matrices S and U it is clear that in addition to a juvenile delay some less obvious mechanisms are present in the size-structured model that can affect the dynamics: the current (age, size)-relation, or growth curve, changes due to a change in the food availability. We will refer to this process as *growth curve plasticity*. This plasticity obviously influences both the feeding and the reproduction of the *Daphnia* population. The importance of the mechanism is somewhat elucidated if we focus upon the prey escape criterion from the unstructured model (Eq. (21)). The prey escape mechanism was the only way that the equilibrium in the unstructured model could become unstable. The criterion (21) stated that the equilibrium in the unstructured model was stable when the food intake rate of the total predator population increased (decreased) faster than the growth rate of the prey with an increase (decrease) in the prey density. If we, for the time being, assume that the same mechanism would also completely determine the stability of the equilibrium in the structured model, we thus have to compare in equilibrium the change in the food intake rate of the total predator population with the change in the growth rate of the prey that would result from a slight change in the prey density. This literal interpretation of the criterion (21) would yield the following stability criterion:

$$\left.\frac{d\bar{A}_f(0)}{dx}\right|_{x=\tilde{x}} > \left.\frac{dR(x)}{dx}\right|_{x=\tilde{x}}, \tag{25}$$

which can be rewritten as

$$\frac{\bar{A}_f(0)f'(\tilde{x})}{f(\tilde{x})} + 2v_x \int_0^{A_{\max}} \tilde{l}(a) l_m f(\tilde{x})(1 - e^{-\gamma a})\tilde{b}F(a)\, da f'(\tilde{x}) > R'(\tilde{x}) \tag{26a}$$

or

$$3\frac{\bar{A}_f(0)f'(\tilde{x})}{f(\tilde{x})} - 2v_x \int_0^{A_{\max}} \tilde{l}(a) l_b e^{-\gamma a}\tilde{b}F(a)\, da f'(\tilde{x}) > R'(\tilde{x}). \tag{26b}$$

It can be shown that taking the limit $\gamma \to \infty$ and $A_{\max} \to \infty$ in the characteristic equation (17) for the structured model and taking the same limit in the criterion (26) yields identical results. We therefore conclude that for $\gamma \to \infty$ and $A_{\max} \to \infty$ the stability of the internal equilibrium is completely determined by criterion (26). In this limiting case we can conceive a neonate *Daphnia* to exhibit an instantaneous jump in

length from its length at birth l_b to its ultimate length $l_m f(x)$, which depends on the current food availability. There hence is no juvenile delay between birth and onset of reproduction and the stability of the equilibrium is entirely governed by the control that the feeding of the *Daphnia* imposes upon the growth of the algae. If we, however, would have used the criterion (21) literally instead of its interpretation and replaced the quantity $v_x l_u^2 \tilde{m}_u$ with its equivalent $\bar{A}_f(0)/f(\tilde{x})$ from the structured model we would have obtained

$$\frac{\bar{A}_f(0) f'(\tilde{x})}{f(\tilde{x})} > R'(\tilde{x}). \tag{27}$$

This inequality only incorporates the direct influences of a change in the prey density upon the total food intake rate of the predator and the growth rate of the prey. The differences between (26) and (27) are exactly due to the influence of the growth curve plasticity upon the feeding behaviour of the population. The inequalities (26a) and (27) suggest that the latter mechanism has a considerable stabilizing influence upon the system. The control of the *Daphnia* population exerted upon the algae is now enhanced, because the growth curve plasticity of the *Daphnia* changes the (age, size)-relation in accordance with the prevailing food availability, which constitutes an indirect way to adjust the feeding rate of the population. From (26b) we infer that this stabilizing influence is maximal for very high values of the growth rate γ. Moreover, it is intuitively clear that the influence of the growth curve plasticity will be larger if the ultimate size can vary over a larger size range. This also follows from the criterion (26).

6. Numerical computations of the stability boundaries

In the previous section we studied the general structure of the characteristic equation (17). This enabled us to distinguish a few mechanisms that are specifically due to the internal size-structure of the *Daphnia* population and the processes on the individual level related to it. As was noted in that section, the internal equilibrium, if it exists, can only become unstable if it merges with a stable or unstable limit cycle when a pair of complex, conjugate roots of (17) cross the imaginary axis from left to right. Numerically we can study this Hopf bifurcation by putting $\lambda = i\omega$ in (17) and solving the resulting complex equation for ω and one free parameter.

For the Kooijman–Metz model applied to *Daphnia magna* all but one of the parameters concerning the individual behaviour of *Daphnia* are experimentally determined with reasonable accuracy. Only the random death rate μ of the individuals is very variable, since it is influenced strongly by the environmental and experimental conditions experienced by the population. For the same reason the growth parameters for the algal food population are very variable. We will therefore solve the complex equation (17) after substitution of $\lambda = i\omega$ to obtain branches of solutions in the parameter plane spanned by the random death rate μ and the maximum algal concentration $X_{\max}$. This procedure will be carried out separately for the two possible growth equations (Eqs. (5a) and (5b)) for the algae.

Figure 2a shows the computed stability boundary in the $(\mu, X_{\max})$-plane for the chemostat algal dynamics (Eq. (5a)) with $\alpha = 0.5$. The second line in the figure represents the existence boundary of the internal equilibrium, defined by $P(X_{\max}) = 1$. For values of $X_{\max}$ above this boundary the internal equilibrium exists. As mentioned before, the equilibrium algal density $\tilde{x}$ equals the value of $X_{\max}$ on this particular boundary. Figure 2b shows the equivalent diagram in case of logistic algal growth

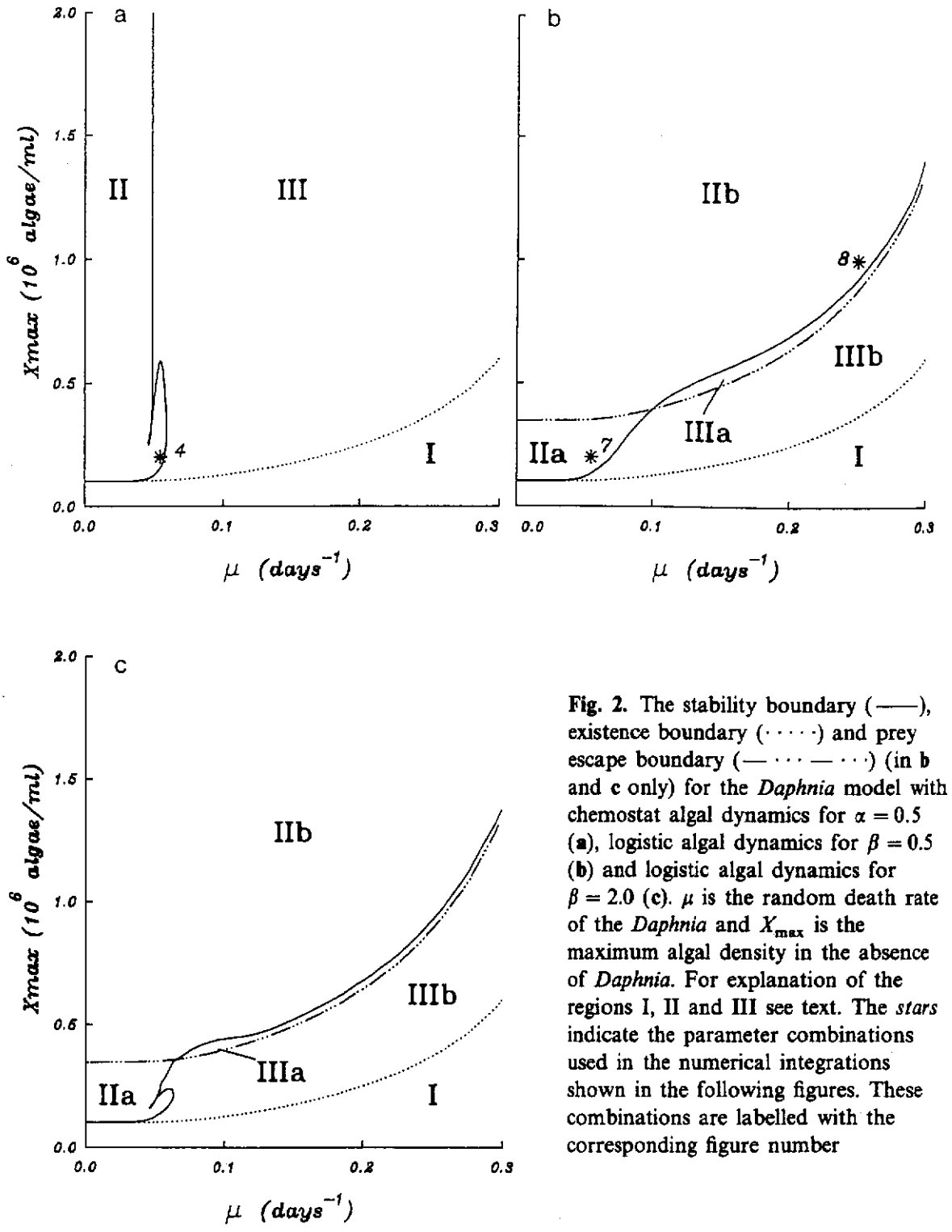

Fig. 2. The stability boundary (——), existence boundary (· · · · ·) and prey escape boundary (— · · · — · · ·) (in **b** and **c** only) for the *Daphnia* model with chemostat algal dynamics for $\alpha = 0.5$ (**a**), logistic algal dynamics for $\beta = 0.5$ (**b**) and logistic algal dynamics for $\beta = 2.0$ (**c**). μ is the random death rate of the *Daphnia* and X_{max} is the maximum algal density in the absence of *Daphnia*. For explanation of the regions I, II and III see text. The *stars* indicate the parameter combinations used in the numerical integrations shown in the following figures. These combinations are labelled with the corresponding figure number

(Eq. (5b)) with $\beta = 0.5$. Again also the existence boundary of the internal equilibrium is drawn.

To compare Figs. 2a and 2b it is instructive to investigate if there are parameter combinations for which the two types of algal dynamics (Eqs. (5a) and (5b)) are comparable. The logistic algal growth equation can also be written as

$$R(x) = \beta \frac{x}{X_{max}} (X_{max} - x), \qquad (5b')$$

and hence for x/X_{max} only slightly smaller than 1 the two types of algal dynamics

seem equivalent. Indeed, if we set $x = X_{max} - \epsilon$ and neglect second and higher order terms in ϵ, Eq. (5b') yields $R(x) = \beta\epsilon$, which matches with $R(x) = \alpha\epsilon$, resulting from setting $x = X_{max} - \epsilon$ in Eq. (5a). Hence, for values of x just below X_{max} the two types of algal dynamics are comparable.

A major difference between the two types of algal dynamics is the absence of the prey escape mechanism in case of the chemostat algal dynamics (Eq. (5a)): because $R'(x)$ is always negative there is no possibility that the algal population can escape the control imposed by the predator (refer to Eqs. (21), (26) and (27)). With logistic algal growth, however, the prey escape mechanism is present. Figure 2b therefore contains an additional third line, given by $\bar{A}_f(0)f'(\tilde{x})/f(\tilde{x}) = R'(\tilde{x})$ (see Eq. (27)). This additional line represents the boundary at which the equilibrium in an unstructured model would become unstable. We paid special attention to the chemostat type of algal dynamics, precisely because it lacks the prey escape mechanism. This type of dynamics enables us to study exclusively the influence of the mechanisms inherent in the size-structure of the *Daphnia* population.

With higher values of α and β the stability diagrams for chemostat and logistic algal dynamics start to display more common characteristics. A larger value of α primarily results in a scaling down of the X_{max}-axis: the peninsula with unstable parameter combinations at low values of X_{max} shrinks, but the vertical asymptote of the stability boundary remains the same. Figure 2c shows for comparison the stability diagram for logistic algal dynamics with the rather high value $\beta = 2.0$. The appearance of a peninsula of instability at low values of X_{max} strongly suggests a relation with the comparable unstable region in case of chemostat algal dynamics (compare Fig. 2a). In the following sections it will be shown that the dynamics of the model exhibited with parameter values in this part of the parameter plane are very similar for both logistic and chemostat algal dynamics.

In view of the above-mentioned similarities and dissimilarities we can distinguish analogous regions in the stability diagrams of the two types of algal dynamics (Fig. 2). Region I is identical for both types of algal dynamics and represents the region in which the internal equilibrium does not exist. In this region $P(X_{max}) < 1$ and hence on average an individual *Daphnia* does not replace itself during its lifetime. The regions II and III represent the parameter combinations which give rise to an unstable and a stable equilibrium, respectively. These regions differ for the two types of algal dynamics. In case of logistic algal growth (Fig. 2b,c) both these regions can be subdivided into two parts: the unstable region II in Fig. 2b,c can be conceived to consist of a region IIa that corresponds to the lower part of the unstable region II from Fig. 2a, and by a region IIb that is apparently due to the prey escape mechanism. We can also distinguish parameter combinations (region IIIa, Fig. 2b,c), for which $\bar{A}_f(0)f'(\tilde{x})/f(\tilde{x}) < R'(\tilde{x})$ (the prey escape boundary from Eq. (27)), while the equilibrium is nonetheless stable. Presumably this is an effect of the stabilizing influence of the growth curve plasticity, as described in the previous section.

The stability diagrams from Fig. 2 give some insight in the relative importance of the mechanisms that were distinguished in the previous section. From Fig. 2b,c we infer that the prey escape mechanism, if present, has a considerable influence upon the stability of the equilibrium. These diagrams suggest that this mechanism accounts for a large proportion of the unstable region in case of logistic algal dynamics: only at low values of μ and low values of X_{max} the prey escape mechanism is second in importance and the stability is more determined by the mechanisms inherent in the life history of *Daphnia*. The latter mechanisms of course determine completely the stability of the equilibrium in case of chemostat algal dynamics.

The separate influences of these mechanisms, i.e., the juvenile delay and the

influences of the growth curve plasticity upon feeding and reproduction, can only be studied in detail using numerical simulations of the dynamics of the model (see following section). However, some clues to their influence can already be inferred from a, rather unconventional, numerical study of the stability equation (17). By subsequently dropping some or all of the terms within braces in Eqs. (17d) and (17e) and solving numerically the stripped equation in the same manner as before we constructed the diagram in Fig. 3. This figure shows, in principle, the same stability diagram as in Fig. 2a with two additional lines: the first additional line (a) resulted from dropping in Eqs. (17d) and (17e) for s_{12} and s_{22}, respectively, all terms within braces which concern the growth curve plasticity. The equation that we study after dropping these terms can be interpreted (see the appendix) as reflecting a situation in which the growth curve always equals the equilibrium growth curve corresponding to the parameter values under consideration: small perturbations in the food availability are assumed not to influence the growth curve. The only destabilizing mechanism that remains is the, now fixed, maturation delay between birth and onset of reproduction. The second additional line (b) resulted from only dropping the terms within braces in Eq. (17e) for s_{22}. These terms concern the influence of the growth curve plasticity upon the feeding of the daphnids. In this case the influence of the growth curve plasticity upon the reproduction is retained.

The results in Fig. 3 suggest that the growth curve plasticity determines to a large extent the stability of the equilibrium, in case of chemostat algal dynamics. Its influence upon the *Daphnia* reproduction seems to have a destabilizing effect, while its influence upon the feeding of the *Daphnia* seems to stabilize the system.

To determine the relative importance of the two separate effects of the growth curve plasticity upon the reproduction (i.e., the change in adult fecundity and the change in juvenile delay), we also computed the branch of solutions in case only the first term within braces in s_{12} (Eq. (17d)) was retained while the other terms within braces in both s_{12} and s_{22} were dropped. This resulted in a line almost equal to line (b), though slightly shifted to the left. We conclude that the shift from line (a) to line (b) by including the influence of the growth curve plasticity upon reproduction is largely due to its effect upon the juvenile delay and only partly to its effect upon the

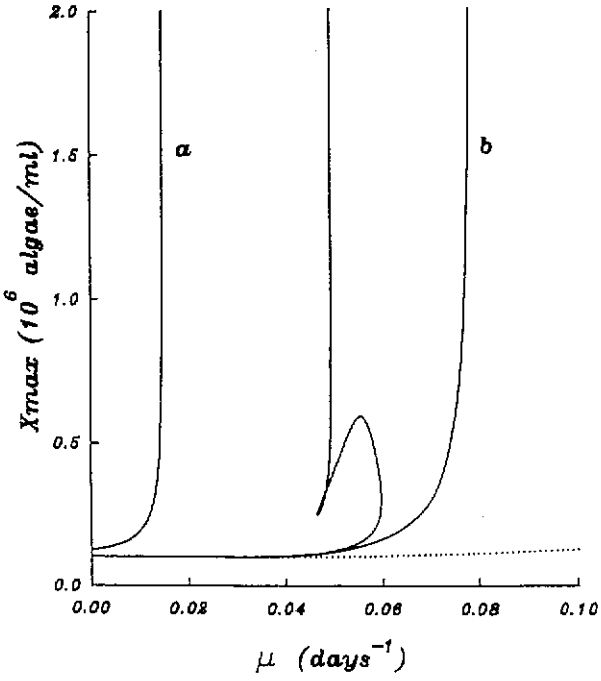

Fig. 3. As Fig. 2a. The additional lines represent the branches of solutions of Eq. (17) when no growth curve plasticity occurs (*a*) and the growth curve plasticity influences reproduction only (*b*)

adult fecundity. Although we cannot make these effects more explicit, the numerical simulations in the next section equally suggest that these two mechanisms are very important for the dynamics of the population.

7. The population dynamics

The dynamics of the model was studied using a recently developed numerical method, called the *Escalator boxcar train* [3, 4], which is specifically tailored for the numerical integration of the equations that occur in physiologically structured population models. These numerical integrations were carried out with many different combinations of the parameters α, μ and X_{max} in case of chemostat algal dynamics and β, μ and X_{max} in case of logistic algal growth. Moreover, the integration runs were frequently repeated with a higher numerical accuracy to rule out the possibility of numerical artefacts. The numerical integration technique turned out to yield very reliable results that were hardly influenced by a change in the integration accuracy.

A large number of the numerical integrations were done to check the correctness of the computed stability boundaries from the previous section. If the initial condition of the system was sufficiently near to the equilibrium state, damped oscillations in the total population sizes of *Daphnia* and algae were observed at the stable and persistent oscillations at the unstable side of the stability boundary. Hence, these numerical integrations confirm the position of the boundary, which inspires some trust in the validity of the stability analysis presented.

7.1. Chemostat algal dynamics

We will first discuss in more detail the dynamic behaviour of the model in case of chemostat algal dynamics with $\alpha = 0.5$. The corresponding stability diagram was already shown in Fig. 2a. The figure also indicates the values of μ and X_{max} that were used in the numerical integrations presented below. These parameter combinations are indicated by means of the figure numbers in which the results of the numerical integrations are shown.

In Fig. 4a the dynamics of both the *Daphnia* and the algae is shown for values of μ and X_{max} within the peninsula of instability jutting out from the main unstable region (Fig. 2a). The oscillations in total *Daphnia* density exhibited in the numerical integration are characterized by a relatively rapid increasing phase and a slower decreasing phase. The amplitude of these fluctuations appears to be larger than the amplitude of the algal oscillations. The phase difference between the oscillations in both populations is approximately 1/2 period between the moments at which both populations attain their minimum density, and approximately 1/4 period at the maximum densities. Figure 4a also indicates the minimum food level below which an individual *Daphnia* would never reach maturity, irrespective of its chance to die before its maximum lifespan. During a large part of the population cycles the food availability drops below this minimum food level for maturation.

The demography of the *Daphnia* population changes quite drastically during one population cycle (Fig. 4b). Juvenile and adult individuals alternately make up a large part of the population. During one complete cycle the *Daphnia* population is apparently dominated by the same cohort of individuals in successive stages of their life history. This dominant cohort is founded at the start of the increasing phase in *Daphnia* density, due to a pulse of reproduction (Fig. 4b). This reproduction pulse is

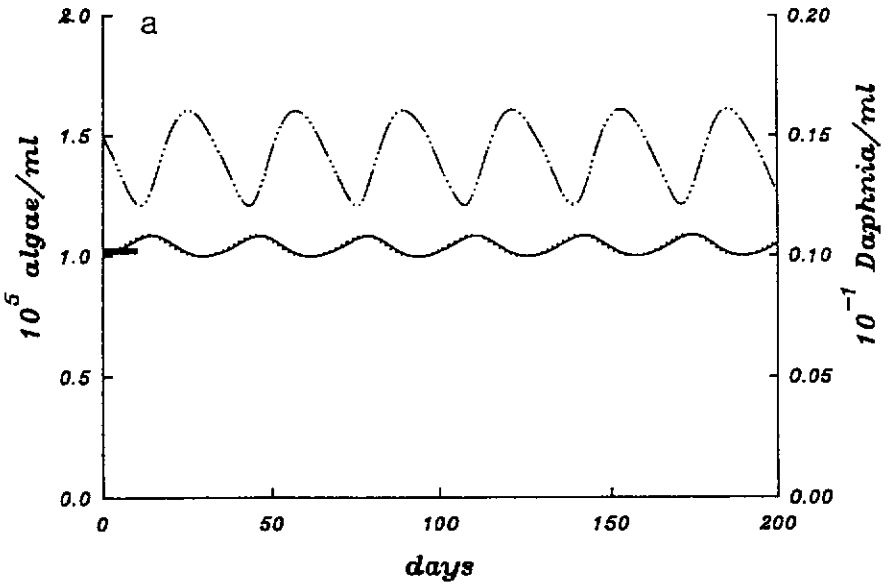
a
2.0
1.5
1.0
0.5
0.0
0.20
0.15
0.10
0.05
0.00
0
50
100
150
200
days
10^5 algae/ml
10^{-1} Daphnia/ml

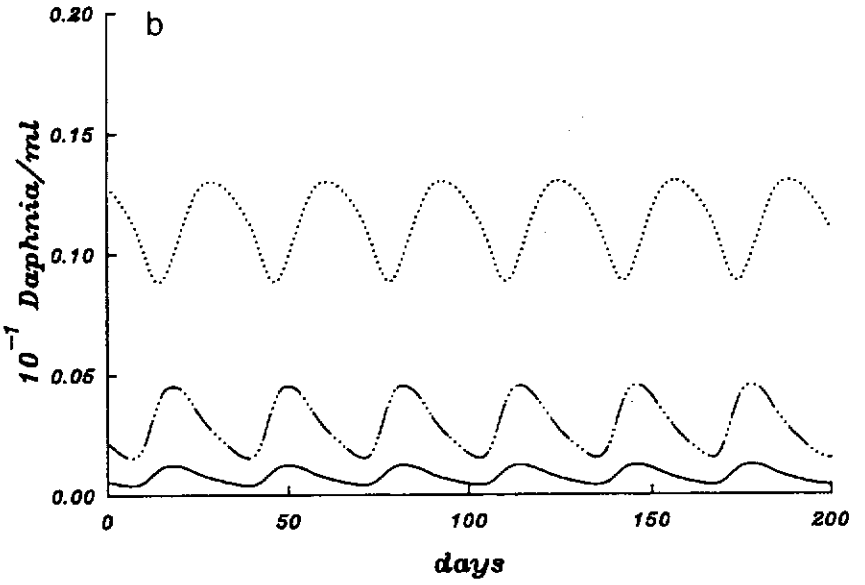
b
0.20
0.15
0.10
0.05
0.00
0
50
100
150
200
days
10^{-1} Daphnia/ml

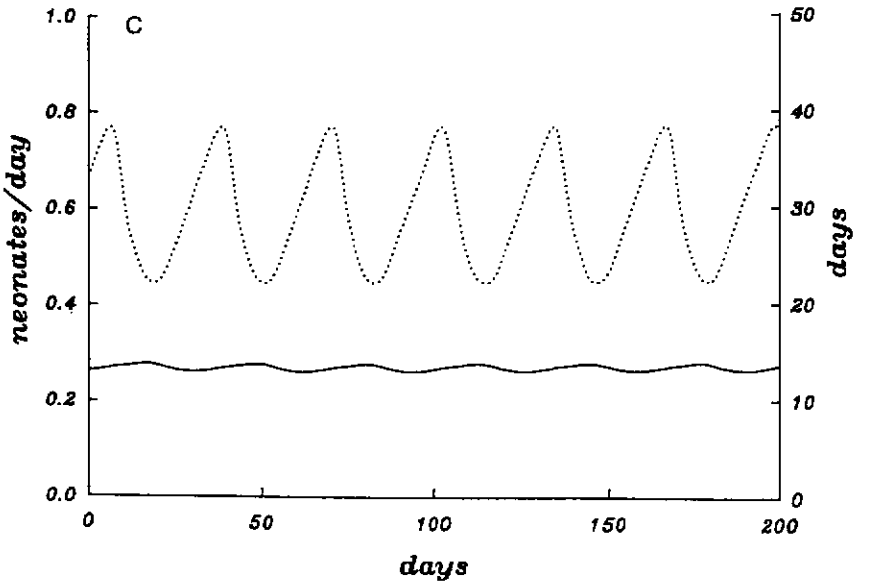
c
1.0
0.8
0.6
0.4
0.2
0.0
50
40
30
20
10
0
0
50
100
150
200
days
neonates/day
days

Fig. 4

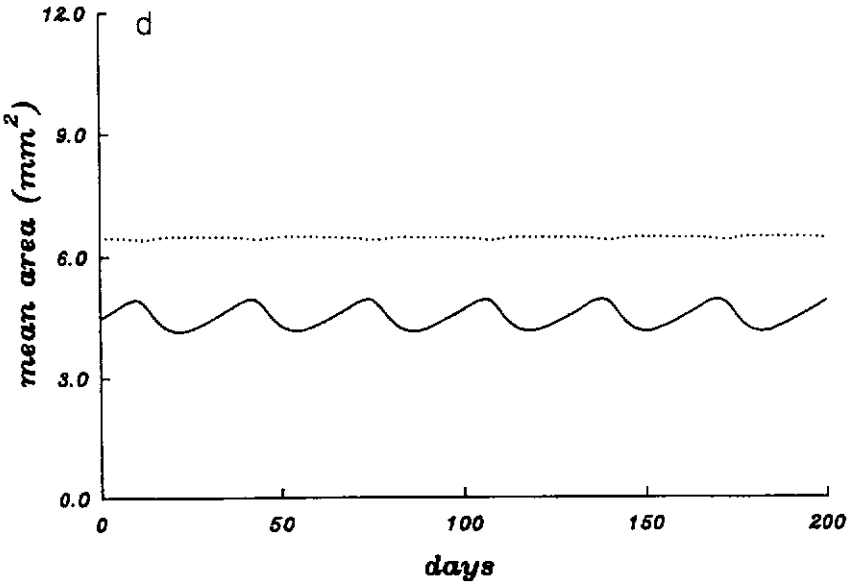

Fig. 4a–d. Dynamical behaviour of the *Daphnia* model with chemostat algal dynamics ($\alpha = 0.5$, $\mu = 0.055$ and $X_{max} = 2.0 \times 10^5$). **a** Simulated *Daphnia* (— · · · —) and algal (——) densities, and PSS agal (· · · · ·) density (see text). The bar at the left axis indicates the minimum algal density for maturation. **b** Population birth rate (——), density of juvenile (· · · · ·) and adult *Daphnia* (— · · · —). **c** Mean fecundity of an adult *Daphnia* (——) and the age of the youngest adult individual, (· · · · ·). **d** Mean individual surface area for the whole *Daphnia* population (——) and for the adult *Daphnia* (· · · · ·) separately

caused by two effects: just prior to the increase in *Daphnia* density the food availability has recovered and reached levels above the minimum level for maturation. This results in (1) an increase in fecundity of the remaining adult *Daphnia* (Fig. 4c) and (2) a burst of juvenile individuals that mature into adults (Fig. 4b). The newly formed cohort of neonates starts growing, but in joint action with their mothers they bring down the food level below the minimum level of maturation. This induces that the growth in size of the formed cohort stops and that the fecundity of their mothers drops. The suppression of the growth in size leads to an increased tightening of the size range of the dominating cohort, while it is still captured in the juvenile phase. This situation lasts till the population has been decimated due to natural mortality and the food availability has recovered. The tightening of the size range of the dominant cohort now induces that the individuals mature almost in one burst. Hence, the cohort almost instantaneously replaces its adult predecessor and initiates a new cycle.

The life history of *Daphnia* obviously plays an important role in the dynamics. Especially the change in the length of the juvenile period with the fluctuations in food availability, the first effect of the growth curve plasticity upon reproduction, seems to have a profound influence. The graph of the age of the youngest adult individuals versus time (Fig. 4c) shows that for a large part of the cycle no maturation at all takes place with a subsequent rapid maturation of all the adolescent individuals present.

The second effect of the growth curve plasticity upon reproduction, i.e., the change in adult fecundity due to a change in the size at every age, has no notable effect (Fig. 4c). Since the observed food levels are only just above the minimum level for maturation the ultimate size that an individual can attain is only slightly above l_j. This implies also that the mean size of the adults is almost constant in time and only slightly larger than l_j. In Fig. 4d this phenomenon is exemplified by plotting the mean surface area of an adult individual versus time. This mean individual surface area is a direct measure of the maximum fecundity of an individual.

The stabilizing influence of the changing individual food intake rate due to the growth curve plasticity shows up in the dynamics of the mean surface area of all the *Daphnia* present (Fig. 4d). This mean area is a direct measure of the maximum feeding capacity of an average individual. The fluctuations in the mean individual surface area are in exact antiphase with the oscillations in *Daphnia* density, thus reducing the impact of these oscillations upon the algal population.

In a previous section we already noted that in case of chemostat algal dynamics the prey escape mechanism was absent. Indeed the contribution of the chemostat algal dynamics to the oscillations is negligible. Even at these low values of X_{max} the algal density is almost equal to the density that would result in case of a pseudo-steady-state (PSS) between the algae and the total grazing surface area of the *Daphnia* (Fig. 4a). This PSS value of the algal density can be calculated from Eq. (8) by setting $dx/dt = 0$ and solving for the food availability x, given the values of the grazing surface area of the *Daphnia* population at that time. The PSS food availability determined in this way can be viewed as set completely by the dynamics within the *Daphnia* population and especially the dynamics of its internal structure. Obviously, the observed algal density tracks the PSS algal density very closely with a negligible influence of the algal growth dynamics: the prey meticulously follows the PSS density which is set by the predator. Note that this dynamical behaviour is essentially different from the usual predator-prey oscillations that occur in unstructured models, due to the phase lag between the populations of approximately 1/2 period.

The numerical integrations that were carried out with chemostat algal dynamics show that at high values of X_{max} the observed food availability is even graphically indiscernible from the PSS food availability. At low values of X_{max} there still exists a tiny influence of the algal dynamics itself (Fig. 4a). Also an increasing value of α results in an observed food availability that is more and more equal to the PSS food availability. These observations can be understood by investigating how quickly the actual algal density approaches the PSS algal density set by the *Daphnia*. The time constant, which characterizes this approach, can be inferred from Eq. (8) by linearization of the equation around the PSS value. It is intuitively clear that this time constant is determined by the value of α and the feeding rate of the total *Daphnia* population. The size of the *Daphnia* population is in turn positively correlated with X_{max} as was seen before. High values of α and/or high values of X_{max} hence result in a large time constant and thus an algal density that very quickly approaches the PSS density. With an increasing value of α the unstable peninsula in the stability diagram is seen to shrivel away, while a decrease in α induces an increase in the size of the peninsula. This leads us to conclude that the unstable peninsula is at least partly the result of the actual algal density lagging behind the PSS algal density. Moreover, the fact that for high values of X_{max} the algal dynamics is completely determined by the *Daphnia* dynamics via the PSS algal density also explains why the stability boundary tends to a vertical asymptote that is independent of the parameters of the chemostat algal dynamics.

The described pattern of oscillation is more or less characteristic for the whole unstable area in chemostat algal dynamics (Fig. 2a). Outside this unstable parameter area the internal equilibrium is stable, as is confirmed by numerical integrations that are started with an initial condition very similar to the equilibrium state. However, when a numerical integration is started with a parameter combination in the (stable) region above the unstable peninsula (Fig. 2a) and an initial condition quite different from the steady-state distribution, a persistent limit cycle behaviour results. In this part of the parameter plane we thus find coexistence of a stable equilibrium and a stable limit cycle. Obviously at the part of the stability boundary bordering this stable

region the Hopf bifurcation that gives rise to the limit cycle behaviour is *subcritical*. The persistent oscillations that occur in this stable region show characteristics similar to those described before (see Fig. 4). The main differences are a smaller (now negligible) discrepancy between the observed food availability and the PSS value of the food availability, a shorter oscillation period and a slightly larger amplitude. The shorter period might be the result of the diminished influence of the algal dynamics, as can be inferred from the similarity between observed and PSS food availability. The larger amplitude is possibly due to the higher *Daphnia* densities that are found with these values of X_{max}.

The analysis of the stability diagram as outlined in Fig. 3 suggested that the stability boundary eventually results from a balance between the opposing influences of the growth curve plasticity upon reproduction and feeding. Consequently these influences counteract each other particularly in the region bordering the stability boundary. For this reason we conjecture that the subcritical Hopf bifurcation is due to the fact that the growth curve plasticity exerts a destabilizing (via the reproduction) as well as a stabilizing influence (via the food intake) upon the system. The latter influence is possibly only effective when the system is in the neighbourhood of its equilibrium state. This conjecture about the cause of the subcritical Hopf bifurcation could in principle be tested by systematically varying the relative effect that the growth curve plasticity has on reproduction and feeding. It should be noted that the occurrence of a subcritical Hopf bifurcation in a biological model is not new (see, for instance, [1] and [19]). However, the fact that the internal structure of the predator population and the growth process related with the structure induces such a subcritical bifurcation is a novelty.

At higher values of X_{max} ($>2.0 \times 10^6$ cells/ml) the Hopf bifurcation even turns out to be more complicated: with parameter values at the stable side of the stability boundary again coexistence of a stable equilibrium and a stable limit cycle is observed, as described above. However, with parameter combinations at the unstable side of the stability boundary two stable limit cycles appear to coexist (Fig. 5). If a numerical integration is started with an initial condition in which there is only one cohort of individuals present, the system tends to a stable limit cycle with all the characteristics described before (Fig. 5a). If a numerical integration is started with an initial condition similar to the (unstable) equilibrium state the system exhibits a different type of cyclic dynamics (Fig. 5b). The limit cycle observed now is characterized by a shorter period and a smaller, more irregular amplitude. For values of X_{max} below 2.0×10^6 cells/ml our numerical studies did not reveal this coexistence of two stable limit cycles.

The shorter period and smaller amplitude of the second limit cycle obviously influence the dynamics of the demographic characteristics of the *Daphnia* population (mean size, fecundity, age at maturation, etc.), but in a relative sense the dynamics seems to bear the same characteristics as described for the long period-large amplitude limit cycle. In the presented numerical integrations (Fig. 5) the ratio between the short period and the long period is about 1/2, although this ratio can be larger with other values of μ and X_{max}, for which coexistence of two stable limit cycles occurs. We have not been able to find an appropriate explanation for the coexistence of the two stable limit cycles in this part of the parameter space ($X_{max} > 2.0 \times 10^6$ cells/ml).

On the basis of extensive numerical integrations in the parameter regions, where coexistence of a stable equilibrium and a stable limit cycle or coexistence of two stable limit cycles is found, we constructed a hypothetical scenario of the type of Hopf bifurcation that occurs at the stability boundary. This hypothesis is summarized in Fig. 6. The same stability and existence boundaries are shown as in Fig. 2a for

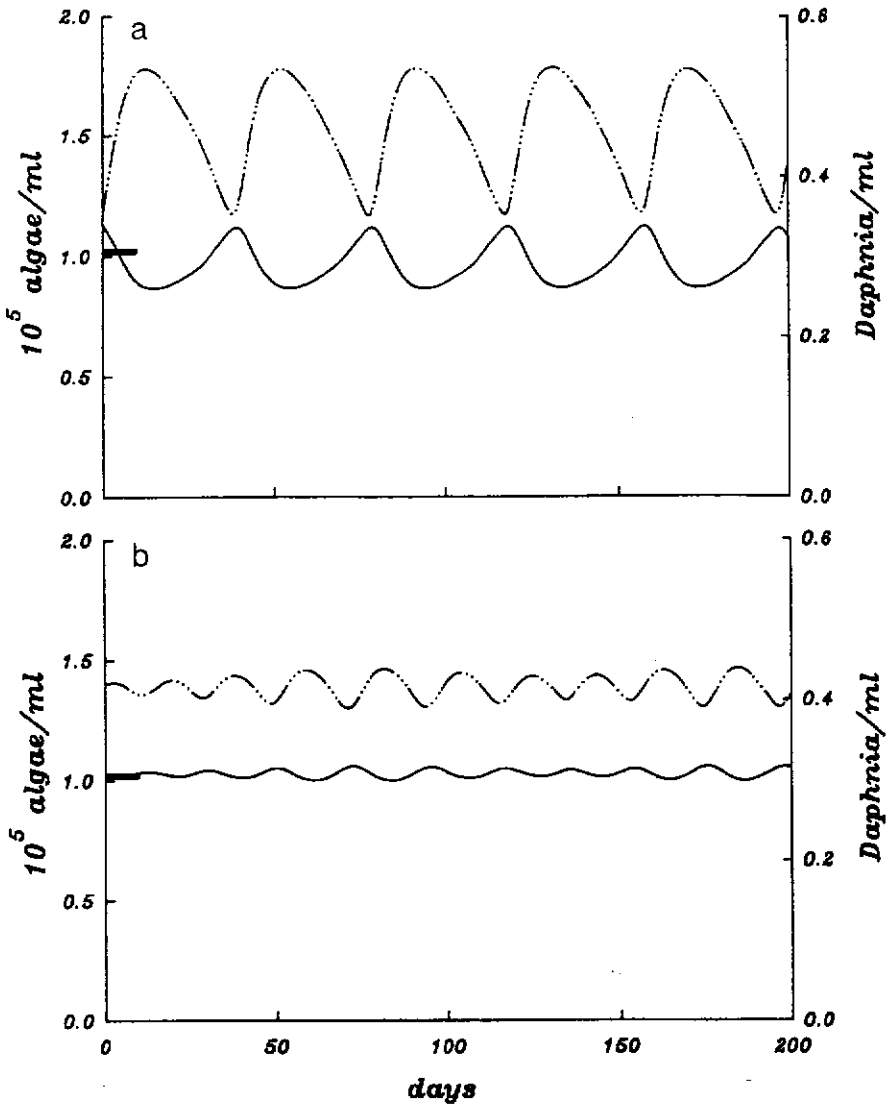

Fig. 5. As Fig. 4a with $\alpha = 0.5$, $\mu = 0.045$ and $X_{max} = 3.0 \times 10^6$ and an initial condition that consists of one cohort of individuals only (**a**) and an initial condition very similar to the equilibrium state (**b**)

$\alpha = 0.5$. In addition, however, we indicate the (approximate) region where coexistence of a stable equilibrium and a stable limit cycle is found. A relatively accurate boundary of a comparable region where coexistence of two stable limit cycles occurs is unfortunately hard to track down with numerical integrations. We do, however, indicate the conjectured type of Hopf bifurcation at the different parts of the boundary. These are depicted by means of qualitative plots, which show (1) the total population size in equilibrium and (2) the way in which this equilibrium merges with a stable or unstable limit cycle (represented by the minimum and maximum population size observed during the cycle). Stable equilibria and limit cycles are always indicated with solid lines, unstable ones with dotted lines. Once again we emphasize that this picture is entirely based on a careful interpretation of numerous numerical integrations. We do not have the technical means to investigate the bifurcations analytically, nor do we know how and why the different conjectured types of bifurcation arise out of each other.

As was noted before, the *Daphnia* population is in general dominated by one cohort of individuals. This means that the oscillations (with the exception of the short period-small amplitude cycles, see below) are of the "single-generation" type

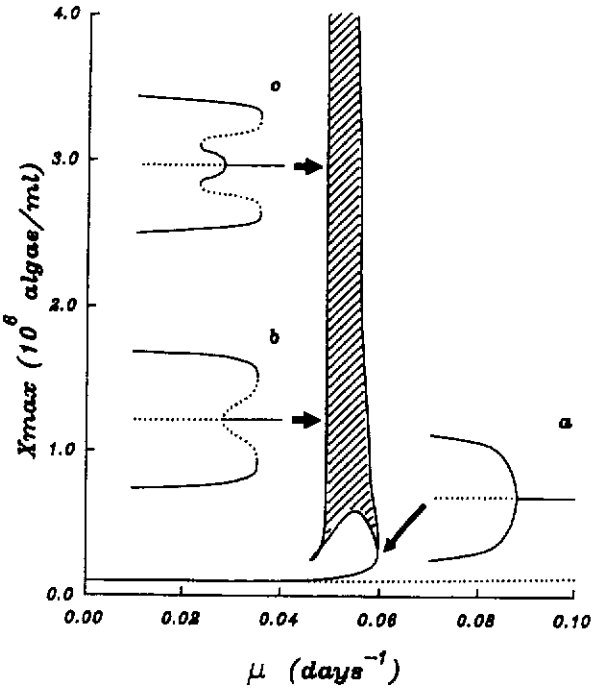

Fig. 6. The (μ, X_{max})-parameter plane for chemostat algal dynamics ($\alpha = 0.5$) with the same stability (——) and existence (· · · ·) boundary as in Fig. 2a. The *shaded area* indicates the region with parameter values for which coexistence of a stable equilibrium and a stable limit cycle occurs. The right-hand boundary of this region is determined on the basis of extensive numerical integrations. The icons *a*, *b* and *c* qualitatively illustrate the type of Hopf bifurcation that occurs at the indicated point of the stability boundary. The horizontal direction in these icons represents the death rate μ, the vertical direction represents the total population size of *Daphnia*. The central horizontal line in each icon qualitatively indicates the total population size in equilibrium as a function of μ. The *curved branches* indicate, again as a function of μ, the maximum and minimum value of the total population size, which occur during the limit cycle arising from the Hopf bifurcation. *Solid lines* for the equilibrium and maximum and minimum population size indicate a stable equilibrium and limit cycle, respectively. *Dotted lines* indicate an unstable equilibrium or limit cycle

described by Nisbet and Gurney [13] (see also [6]). These authors argue that these "single-generation" cycles arise when changes in the number of juveniles present have an immediate effect upon the adult recruitment. This happens, for example, if the time lag between the birth of an individual and the onset of its reproduction depends on the number of juveniles present. In our model an increase in the juvenile density indeed induces such an increase in the time till maturation. Particularly this maturation delay and the changes therein seem to be the driving factor of the observed oscillations. The presented results suggest, however, that the tightening of the size range of the dominant cohort, which occurs during the slowing down of juvenile growth, is also a very important mechanism that adds to the oscillatory tendency.

These remarks are not at all true for the short period-small amplitude cycles that can arise with values of $X_{max} > 2.0 \times 10^6$ cells/ml in case of the coexistence of two stable limit cycles. The period length is considerably shorter than the (mean) time lag between the birth of an individual and the onset of its reproduction. Hence the oscillations cannot be of the "single-generation" type. Obviously these oscillations are due to a density dependent regulation within one generation, although the nature of this regulation is unclear to us.

7.2. Logistic algal dynamics

The stability diagram for logistic algal dynamics was shown in Fig. 2b for $\beta = 0.5$. This stability diagram also shows the parameter combinations of the numerical integrations presented below. These combinations are labelled in the same way as explained in the previous section on chemostat algal dynamics. Figure 7 shows the dynamic behaviour of the *Daphnia* and algal populations with values of μ and X_{max} which equal the parameter values used for the numerical integration from Fig. 4 with chemostat algal dynamics. In general, we can conclude that the observed dynamics with logistic algal growth at these parameter values (Fig. 7) resembles the results with chemostat algal dynamics (Fig. 4).

Especially the demography of the *Daphnia* population during a cycle shows the same pattern under the two types of agal dynamics (compare Figs. 4b and 7b). Obviously the prey escape mechanism, which constitutes the main difference between logistic and chemostat algal dynamics, is not very important yet. Hence, with low values of μ and X_{max} the life history of *Daphnia* always determines to a large extent

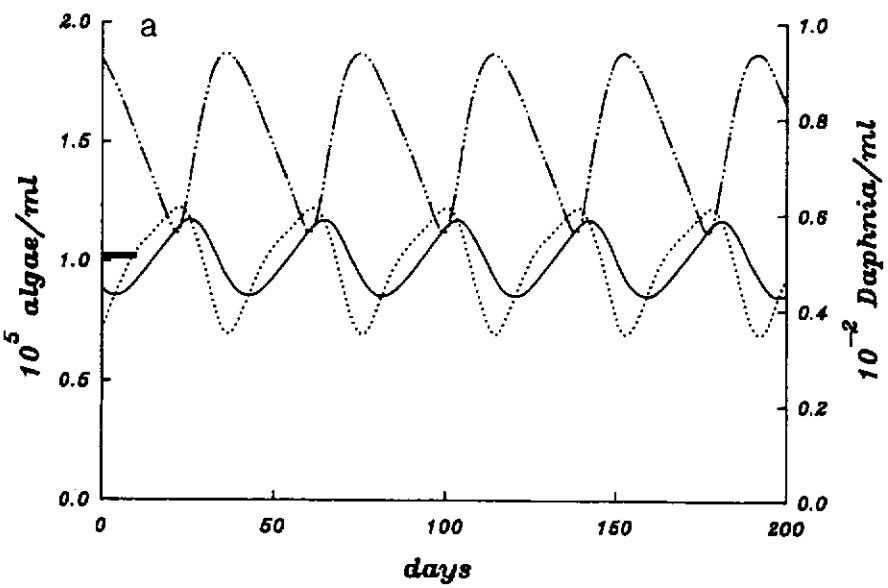

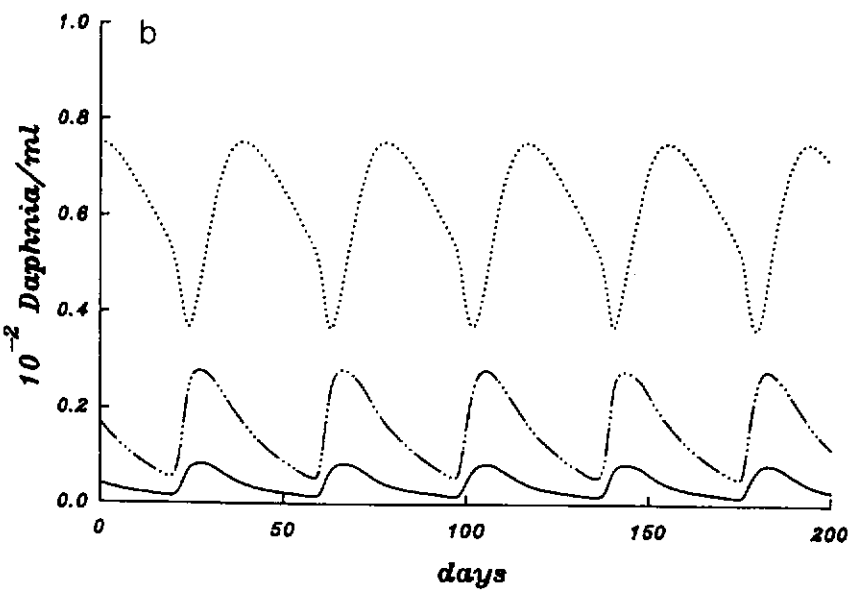

Fig. 7

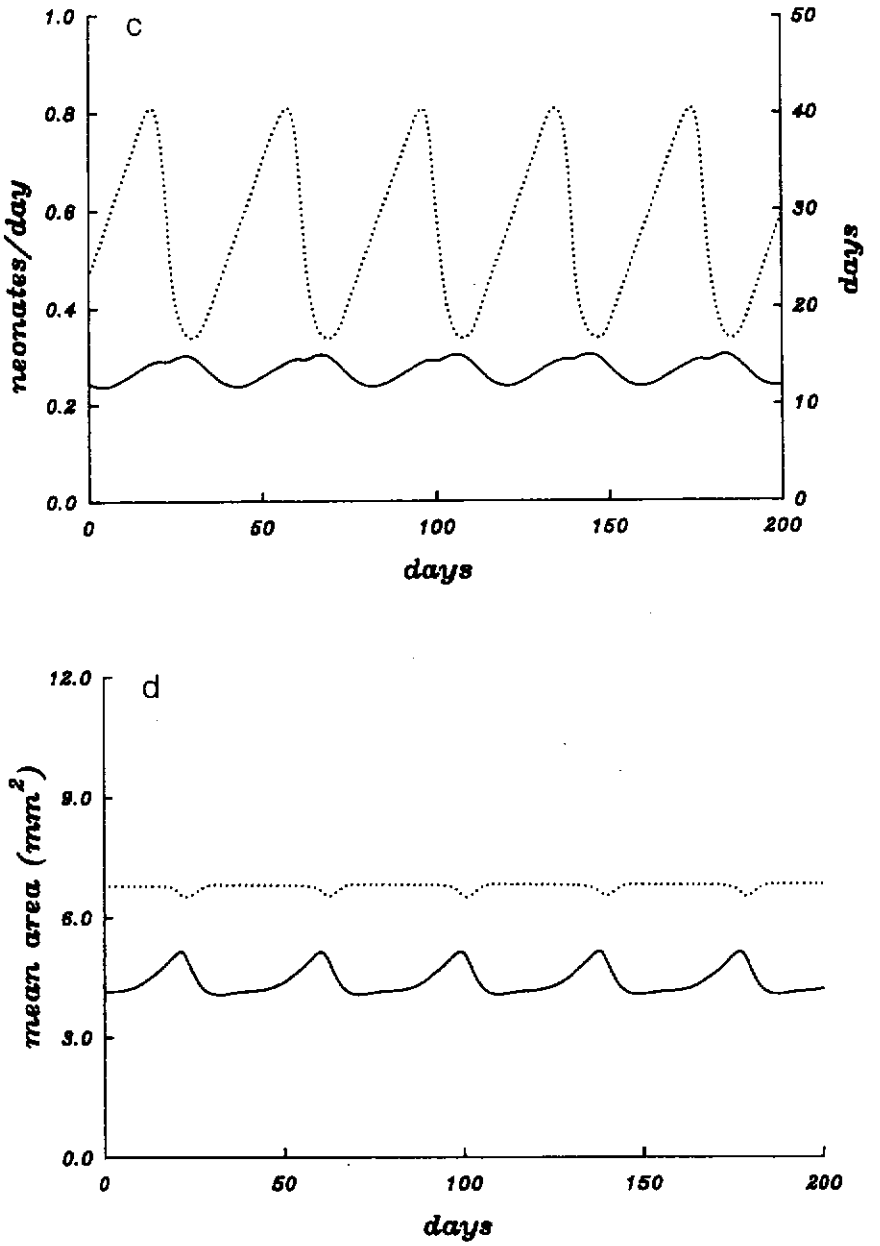

Fig. 7. As Fig. 4, but now for logistic algal growth with $\beta = 0.5$, $\mu = 0.055$ and $X_{max} = 2.0 \times 10^5$

the oscillatory behaviour, irrespective of the type of algal dynamics. Some influence of the logistic algal growth can be seen in the larger discrepancy between the PSS and the observed algal density (Fig. 7a), the larger fluctuations in the adult fecundity (Fig. 7c) and the lower overall density of *Daphnia* (Fig. 7a). Nonetheless, during one cycle the population is again dominated by one cohort of individuals in successive stages of its development.

In Fig. 8a the dynamics of both the *Daphnia* and the algae is shown for a high value of μ and a high value of X_{max}. This dynamics is very different from those presented before. Some eye-catching properties are the larger amplitude of the algal fluctuations in comparison with the *Daphnia* fluctuations and the phase lag between algae and *Daphnia*. The *Daphnia* lag behind by about 1/4 period at their population minimum and by about 1/3 period at their maximum. The demography of the *Daphnia* population during the oscillations (Fig. 8b) suggests that with these parameter values the life history characteristics of *Daphnia* hardly play any role. The relative proportion of juvenile versus adult *Daphnia* is more or less constant during a cycle,

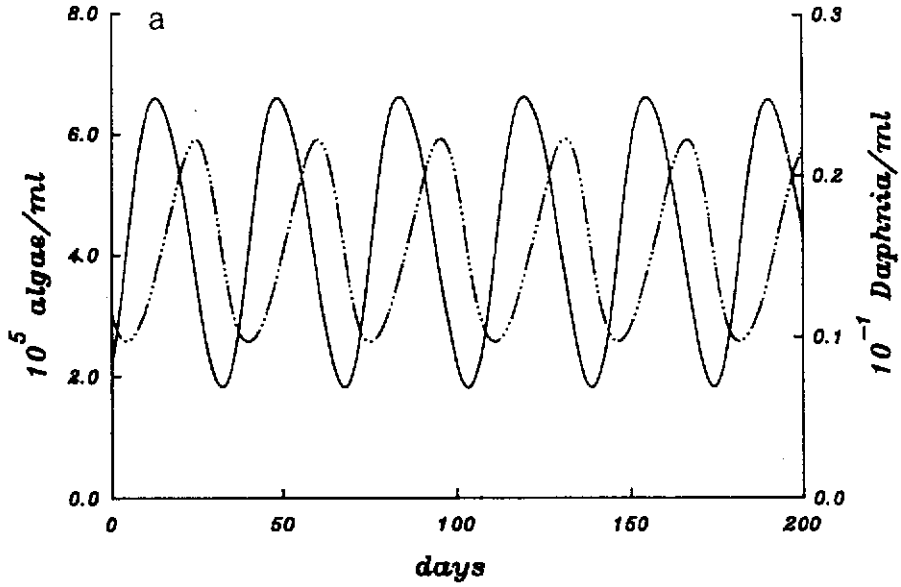
a
8.0
6.0
4.0
2.0
0.0
0.3
0.2
0.1
0.0
0
50
100
150
200
days
10^5 algae/ml
10^{-1} Daphnia/ml

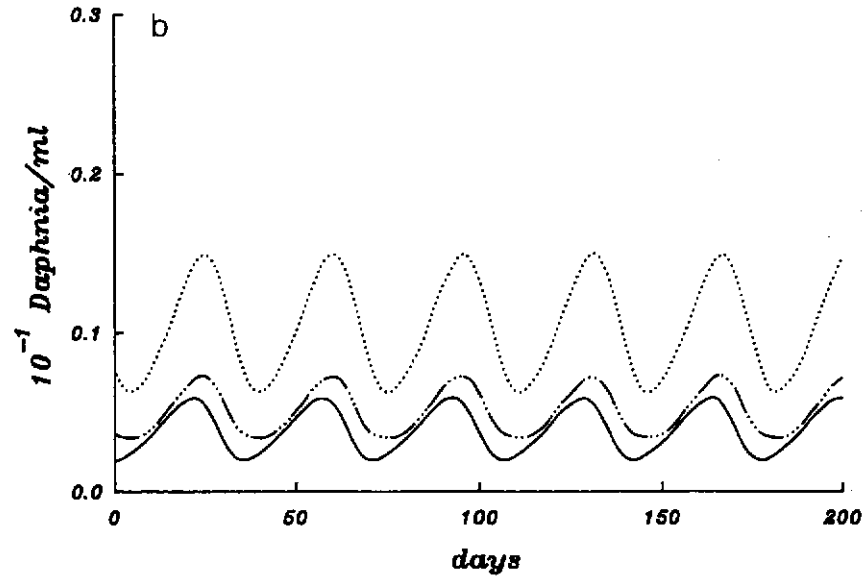
b
0.3
0.2
0.1
0.0
0
50
100
150
200
days
10^{-1} Daphnia/ml

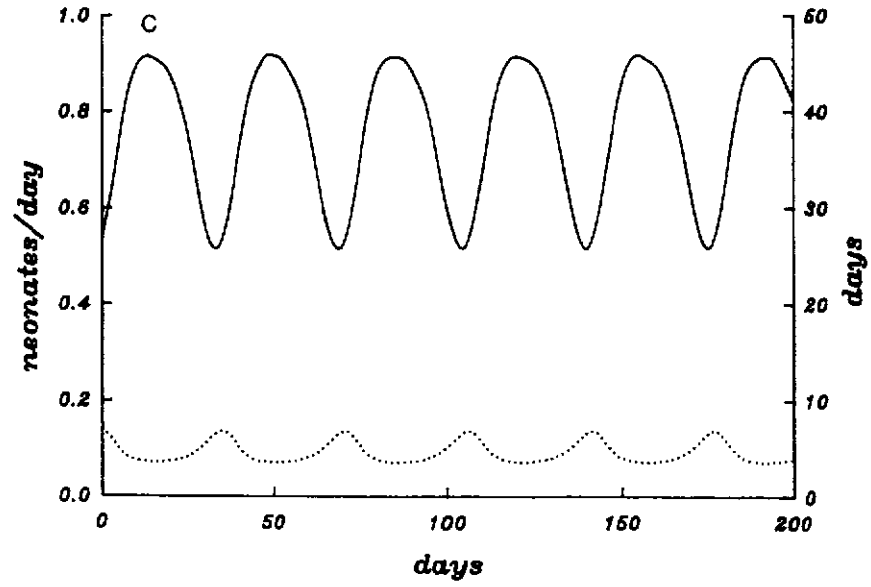
c
1.0
0.8
0.6
0.4
0.2
0.0
60
40
30
20
10
0
0
50
100
150
200
days
neonates/day
days

Fig. 8

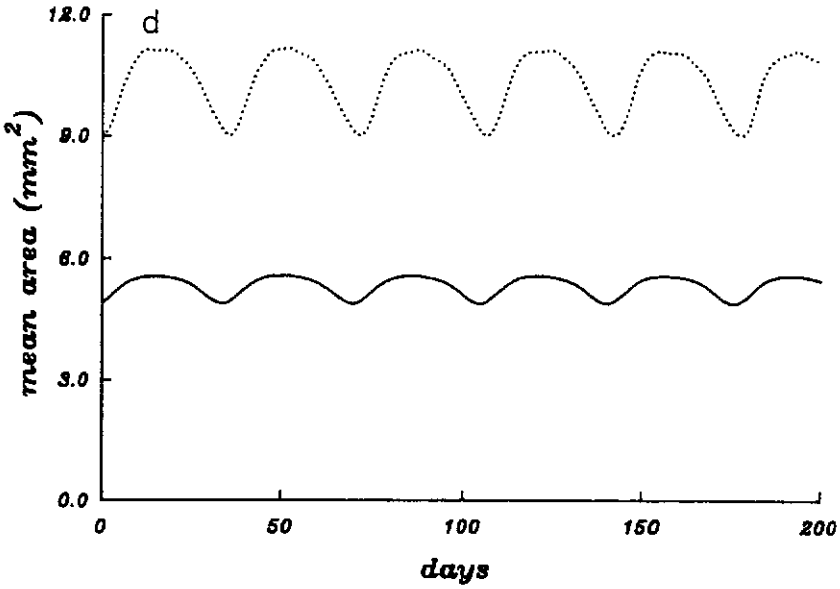

Fig. 8. As Fig. 4, but now for logistic algal growth with $\beta = 0.5$, $\mu = 0.25$ and $X_{max} = 1.0 \times 10^6$

while the population birth rate is also almost in phase with the total population fluctuations.

The high food densities that are found with these parameter values result in a rapid growth in size during an individual's lifetime and hence in a very short juvenile period (Fig. 8c). In contrast with the observations in the previous section, the mean surface area of an adult individual now fluctuates strongly (Fig. 8d). These fluctuations moreover coincide exactly with the fluctuations in food availability (Fig. 8a) and hence result in large fluctuations in adult fecundity during a cycle (Fig. 8c). For these parameter values the dynamics are primarily driven by the adult fecundity as opposed to the delay-driven dynamics discussed in the previous section.

The observed dynamics resembles the dynamics exhibited by the unstructured Lotka–Volterra type models of a predator-prey interaction (such as specified by Eqs. (18)). In particular, the larger amplitude of the prey population and the phase lag between predator and prey of appoximately 1/4 period should be mentioned. Altogether these observations support the earlier hypothesis that in part IIb of the parameter space from Fig. 2b the prey escape mechanism plays an important role.

An oscillation cycle is initiated as the algae escape the control imposed by the *Daphnia*, since the reaction of the latter in terms of feeding is slower than the increase in algal growth rate. The algal density rises, which induces an increase in fecundity of the adult *Daphnia* and a subsequent increase in *Daphnia* density. This increase is, however, overcompensative and causes the algal density to decrease strongly. The fecundity of the adult *Daphnia* drops again and so does the total population size. This leads to the onset of the next cycle. With a change from high values of μ and X_{max} to low values the algae and *Daphnia* thus seem to exchange roles: in the first case the *Daphnia* population clearly pursues the algae, while in the second case the algal population passively follows the regime set by the dynamics of the *Daphnia*.

When numerical integrations are carried out with intermediate values of μ and X_{max} the prey escape mechanism and the life history of *Daphnia* both determine to some extent the dynamics of the system. With a change from high to low parameter values we actually observe a shift in importance from the prey escape mechanism to the life history of *Daphnia* as the determining factor.

In case of logistic algal growth with $\beta = 0.5$ always a supercritical Hopf bifurcation is found at the stability boundary. Comparing the stability diagrams for the chemostat and logistic algal dynamics from Fig. 2, this is also to be expected: with $\beta = 0.5$ the prey escape mechanism already dominates the dynamics in the parameter region where a subcritical Hopf bifurcation could occur. In case β equals 2.0, however, we do find a region just above the unstable peninsula (Fig. 2c) where a subcritical Hopf bifurcation occurs. Here the influence of the prey escape mechanism is not yet that important and coexistence of a stable equilibrium and a stable limit cycle and even of two stable limit cycles is found.

All these numerical integrations were carried out with parameter values from the unstable region in the neighbourhood of the stability boundary. With values further away from this boundary the dynamics becomes very irregular or even chaotic. In these cases the more unrealistic aspects of the model strongly influence the dynamics, since, for example, death from starvation is starting to play a role in contrast with the dynamics of the system near the stability boundary. We therefore have not focussed upon this irregular dynamic behaviour of the model.

8. Concluding remarks

In this paper we have investigated the possible effects of the internal structure of a population upon its dynamics. We have tried to disentangle the influences upon the population dynamics of the various mechanisms that were incorporated in the model for the individual behaviour of *Daphnia*. A quite complicated pattern resulted. The methods that we used are by no means well established. Much of the theory, used implicitly in our formal stability analysis, is not yet built on a rigorous basis, but the fact that the relations between mechanisms and dynamics are confirmed when following several different routes of investigation leads us to accept them.

Another point is that the relations between the observed characteristics of the dynamics with the underlying mechanisms on the individual level are by no means corroborated by experimental evidence. Moreover, in real populations individuals which do not notably differ in their physiological state often display differences in their behaviour. This non-deterministic variation can obscure the causal relations or even weaken the effects on stability of the internal predator (age, size)-dynamics. Hence, the sketched image of relations is not more than a hypothetical one. Although a large body of experimental observations on *Daphnia* population dynamics is available (see [8] for an overview) this study poses a lot of new questions to be verified. Already this generating of new hypothesis is in our opinion a valuable result of the model analysis.

Acknowledgements. We like to thank Mrs. Zitman-de Graaf for typing the first draft of this manuscript. The research of the first author was supported by the Foundation for Fundamental Biological Research (BION), which is subsidized by the Netherlands Organization for the Advancement of Research (NWO).

Appendix

In this appendix we will present the derivation of the characteristic equation (17). This derivation is not at all straightforward, since (a) the growth function g (Eq. (2)) is not differentiable in $l = l_m f(x)$, (b) the reproduction function b (Eq. (3)) is

discontinuous in $l = l_j$ and not differentiable for $l = l_m f(x)$ and (c) the death rate d is discontinuous for $a = A_{\max}$ and $l = l_m f(x)/\kappa$. For these reasons we outline the analysis in detail. We start with defining a small perturbation from the equilibrium state $(\tilde{x}, \tilde{m}(a), \tilde{l}(a))$ as follows:

$$\begin{aligned} \epsilon_x(t) &:= x(t) - \tilde{x}, \\ \epsilon_m(t, a) &:= m(t, a) - \tilde{m}(a), \\ \epsilon_l(t, a) &:= l(t, a) - \tilde{l}(a). \end{aligned} \tag{A1}$$

We will derive a system of linear equations for the dynamics of such a small perturbation to determine the stability of the internal equilibrium. As before we will not always write the arguments of all functions in full, if the context makes clear what these arguments are. Linearization and substitution of exponential trial solutions for the small perturbations ϵ_x, ϵ_m and ϵ_l will be carried out using the system of Eqs. (7), in combination with the ordinary differential equation (8) describing the dynamics of the algal food population.

First we make the important assumption that

$$g(\tilde{x} + \epsilon_x, \tilde{l}(a) + \epsilon_l) > 0, \quad \text{for all } \epsilon_x(t), \epsilon_l(t, a). \tag{A2}$$

Since we assume that the perturbations from the equilibrium state are small, we may expand the function g in terms of ϵ_x and ϵ_l and neglect all terms of second and higher order. In first approximation the assumption (A2) is then equivalent with

$$\epsilon_l(t, a) - l_m f'(\tilde{x})\epsilon_x(t) < l_m f(\tilde{x}) - \tilde{l}(a) \quad \text{for all } \epsilon_x(t), \epsilon_l(t, a). \tag{A3}$$

The assumption (A2) is seen to hold good only if ϵ_x and ϵ_l are sufficiently small for all t and only if $A_{\max} < \infty$. The latter inequality is crucial for the (age, size)-relation in equilibrium to stay bounded away from $l_m f(\tilde{x})$, the ultimate length under the current food availability. This ultimate length is also the threshold value at which rechannelling of ingested energy to cover maintenance requirements starts to play a role (see Eqs. (2) and (3)). The assumption (A2) hence implies that this rechannelling of ingested energy and therefore also death of starvation does not occur in the linearized problem. For this reason we can assume the following formulations for the functions I, g, b and d in the neighbourhood of the equilibrium state:

$$\begin{aligned} I(x, l) &= v_x f(x) l^2 && \text{for } l_b \leqslant l < l_m f(\tilde{x}), \\ g(x, l) &= \gamma(l_m f(x) - l) && \text{for } l_b \leqslant l < l_m f(\tilde{x}), \\ b(x, l) &= r_m f(x) l^2 && \text{for } l_j \leqslant l < l_m f(\tilde{x}), \\ d(x, a, l) &= \mu && \text{for } 0 \leqslant a < A_{\max}. \end{aligned} \tag{A4}$$

These functions are clearly differentiable within their domain of definition. For our local linearization around the equilibrium state $(\tilde{x}, \tilde{m}(a), \tilde{l}(a))$ we can thus neglect the undifferentiable points in the original formulae for the functions g, b and d.

The equalities (A1) are subsequently used to replace the quantities $x(t)$, $m(t, a)$ and $l(t, a)$ in the system of Eqs. (7). However, since the age at which the reproduction starts, occurs in the side condition (7b) and since this age at maturation depends on the food availability, we introduce another perturbation quantity ϵ_a that indicates the perturbation of the age at maturation from its equilibrium value $A_j(\tilde{x})$. This

quantity ϵ_a can be related to the perturbation quantity ϵ_l:

$$\begin{aligned} l_j &= l(t, A_j(\tilde{x}) + \epsilon_a) = \tilde{l}(A_j(\tilde{x}) + \epsilon_a) + \epsilon_l(t, A_j(\tilde{x}) + \epsilon_a) \\ &\approx \tilde{l}(A_j(\tilde{x})) + \frac{\partial \tilde{l}(A_j(\tilde{x}))}{\partial a}\epsilon_a + \epsilon_l(t, A_j(\tilde{x})) \qquad \text{(A5)} \\ \Rightarrow\ \epsilon_a &= \frac{-\epsilon_l(t, A_j(\tilde{x}))}{g(\tilde{x}, l_j)}. \end{aligned}$$

After substitution of the quantities $x(t)$, $m(t, a)$ and $l(t\,a)$, we expand all the functions in terms of the perturbation quantities ϵ and obtain the following linearized system of equations. In this system all terms of second and higher order are consequently neglected:

$$\frac{\partial \epsilon_m}{\partial t} + \frac{\partial \epsilon_m}{\partial a} = -\mu \epsilon_m(t, a), \qquad \text{(A6a)}$$

$$\epsilon_m(t, 0) = \int_{A_j(\tilde{x})}^{A_{\max}} b(\tilde{x}, \tilde{l})\epsilon_m + b_x(\tilde{x}, \tilde{l})\tilde{m}(a)\epsilon_x + b_l(\tilde{x}, \tilde{l})\tilde{m}(a)\epsilon_l\, da - b(\tilde{x}, l_j)\tilde{m}(A_j(\tilde{x}))\epsilon_a, \qquad \text{(A6b)}$$

$$\frac{\partial \epsilon_l}{\partial t} + \frac{\partial \epsilon_l}{\partial a} = g_x(\tilde{x}, \tilde{l})\epsilon_x + g_l(\tilde{x}, \tilde{l})\epsilon_l, \qquad \text{(A6c)}$$

$$\epsilon_l(t, 0) = 0. \qquad \text{(A6d)}$$

The functions g_x, g_l, b_x and b_l indicate the partial derivatives of the functions $g(x, l)$ and $b(x, l)$ with respect to x and l, respectively. Equation (A6b) is derived from the linearization of the original side condition (7b). Especially this part of the linearization procedure is not straightforward and therefore presented here in more detail. Starting with the side condition (7b), Eq. (A6b) is obtained as follows:

$$\begin{aligned} \epsilon_m(t, 0) &= \int_{A_j(\tilde{x})+\epsilon_a}^{A_{\max}} b(\tilde{x} + \epsilon_x, \tilde{l}(a) + \epsilon_l)(\tilde{m}(a) + \epsilon_m)\, da - \tilde{m}(0) \\ &\approx \int_{A_j(\tilde{x})}^{A_{\max}} b(\tilde{x} + \epsilon_x, \tilde{l}(a) + \epsilon_l)(\tilde{m}(a) + \epsilon_m)\, da - \tilde{m}(0) - b(\tilde{x}, l_j)\tilde{m}(A_j(\tilde{x}))\epsilon_a \\ &\approx \int_{A_j(\tilde{x})}^{A_{\max}} b(\tilde{x}, \tilde{l})\epsilon_m + b_x(\tilde{x}, \tilde{l})\tilde{m}(a)\epsilon_x + b_l(\tilde{x}, \tilde{l})\tilde{m}(a)\epsilon_l\, da - b(\tilde{x}, l_j)\tilde{m}(A_j(\tilde{x}))\epsilon_a. \end{aligned} \qquad \text{(A7)}$$

This derivation particularly shows how the perturbation in the age at maturation is accounted for in the linearized system of Eqs. (A6).

Carrying out the same substitution and expansion procedure for the ODE (8) as was done for the system of Eqs. (7) results in the linearized ODE:

$$\begin{aligned} \frac{d\epsilon_x}{dt} &= R(\tilde{x} + \epsilon_x) - \int_0^{A_{\max}} I(\tilde{x} + \epsilon_x, \tilde{l} + \epsilon_l)(\tilde{m} + \epsilon_m)\, da \\ &\approx R'(\tilde{x})\epsilon_x - \int_0^{A_{\max}} I(\tilde{x}, \tilde{l})\epsilon_m + I_x(\tilde{x}, \tilde{l})\tilde{m}(a)\epsilon_x + I_l(\tilde{x}, \tilde{l})\tilde{m}(a)\epsilon_l\, da, \end{aligned} \qquad \text{(A8)}$$

which, in combination with the equations in (A6), constitutes the complete, linearized set of equations of our model. In Eq. (A8) $R'(x)$ denotes the derivative of $R(x)$, while I_x and I_l denote the partial derivatives of $I(x, l)$ with respect to x and l, respectively.

To derive a characteristic equation in the complex variable λ, we next substitute the exponential trial solutions:

$$\begin{aligned} \epsilon_x(t) &:= \Delta_x e^{\lambda t}, \\ \epsilon_m(t, a) &:= \Delta_m(a) e^{\lambda t}, \\ \epsilon_l(t, a) &:= \Delta_l(a) e^{\lambda t}, \\ \epsilon_a &:= \Delta_a e^{\lambda t}. \end{aligned} \tag{A9}$$

into (A6) and (A8), which leads to

$$\frac{\partial \Delta_m}{\partial a} = -(\mu + \lambda)\Delta_m, \tag{A10a}$$

$$\Delta_m(0) = \int_{A_j(\tilde{x})}^{A_{\max}} b(\tilde{x}, \bar{l})\Delta_m + b_x(\tilde{x}, \bar{l})\tilde{m}(a)\Delta_x + b_l(\tilde{x}, \bar{l})\tilde{m}(a)\Delta_l \, da - b(\tilde{x}, l_j)\tilde{m}(A_j(\tilde{x}))\Delta_a, \tag{A10b}$$

$$\frac{\partial \Delta_l}{\partial a} = g_x(\tilde{x}, \bar{l})\Delta_x + g_l(\tilde{x}, \bar{l})\Delta_l - \lambda\Delta_l, \tag{A10c}$$

$$\Delta_l(0) = 0, \tag{A10d}$$

$$\lambda\Delta_x = R'(\tilde{x})\Delta_x - \int_0^{A_{\max}} I(\tilde{x}, \bar{l})\Delta_m + I_x(\tilde{x}, \bar{l})\tilde{m}(a)\Delta_x + I_l(\tilde{x}, \bar{l})\tilde{m}(a)\Delta_l \, da. \tag{A10e}$$

Using the formulas for the functions I, g, b and d as given by Eq. (A4) and the partial derivatives that can be derived from these formulae:

$$\begin{aligned} I_x(x, l) &= v_x f'(x)[l(a)]^2, & I_l(x, l) &= 2v_x f(x) l(a), \\ g_x(x, l) &= \gamma l_m f'(x), & g_l(x, l) &= -\gamma, \\ b_x(x, l) &= r_m f'(x)[l(a)]^2, & b_l(x, l) &= 2r_m f(x) l(a), \end{aligned} \tag{A11}$$

the differential equations (A10a) and (A10c) for $\Delta_m(a)$ and $\Delta_l(a)$ can be solved explicitly. We can therefore express the quantities $\Delta_m(a)$, $\Delta_l(a)$ and Δ_a (see Eq. (A5)) in terms of Δ_x and Δ_b, which we write instead of $\Delta_m(0)$:

$$\begin{aligned} \Delta_m(a) &= \Delta_b F(a) e^{-\lambda a}, \\ \Delta_l(a) &= \frac{\gamma l_m f'(\tilde{x})}{\lambda + \gamma}(1 - e^{-(\lambda+\gamma)a})\Delta_x, \\ \Delta_a &= \frac{-\Delta_l(A_j(\tilde{x}))}{g(\tilde{x}, l_j)} = \frac{-l_m f'(\tilde{x})}{(l_m f(\tilde{x}) - l_j)} \frac{1 - e^{-(\lambda+\gamma)A_j(\tilde{x})}}{\lambda + \gamma} \Delta_x. \end{aligned} \tag{A12}$$

When we now substitute the formulas for the functions I, g, b and d (A4) and their partial derivatives (A11) and the equalities (A12) into the two remaining Eqs. (A10b) and (A10e) we directly end up with the characteristic equation (17). This completes our derivation.

As a last point we show the explicit results of the substitutions into the last two terms of the Eq. (A10b):

$$-b(\tilde{x}, l_j)\tilde{m}(A_j(\tilde{x}))\Delta_a = \frac{r_m f(\tilde{x}) l_m f(\tilde{x}) l_j^2}{(l_m f(\tilde{x}) - l_j)} \bar{b} F(A_j(\tilde{x})) \frac{1 - e^{-(\lambda+\gamma)A_j(\tilde{x})}}{\lambda + \gamma} \frac{f'(\tilde{x})}{f(\tilde{x})} \Delta_x, \quad \text{(A13a)}$$

$$\int_{A_j(\tilde{x})}^{A_{\max}} b_l(\tilde{x}, \bar{l})\tilde{m}(a)\Delta_l \, da = 2\gamma r_m f(\tilde{x}) l_m f(\tilde{x}) \int_{A_j(\tilde{x})}^{A_{\max}} \bar{l}(a)\bar{b}F(a) \frac{1 - e^{-(\lambda+\gamma)a}}{\lambda + \gamma} da \frac{f'(\tilde{x})}{f(\tilde{x})} \Delta_x . \quad \text{(A13b)}$$

The quantity Δ_a denoted a deviation from the equilibrium value of the age at maturation, which was directly related to Δ_l (see (A5) and (A12)). The quantity Δ_l represents a deviation from the equilibrium (age, size)-relation that was in turn related to a deviation from the equilibrium food availability, according to (A12). The equalities (A13) therefore show that the braced terms in the element s_{12} of the characteristic equation indeed concern the influence of the growth curve plasticity upon reproduction. The first braced term in (17d), which is derived in Eq. (A13a), reflects the influence of the growth curve plasticity upon the age of maturation, while the second braced term in (17d) reflects the influence upon adult fecundity. Similarly the explicit result of the substitutions into the last term of (A10e) is

$$\int_0^{A_{\max}} I_l(\tilde{x}, \bar{l})\tilde{m}(a)\Delta_l \, da = 2\gamma v_x f(\tilde{x}) l_m f(\tilde{x}) \int_0^{A_{\max}} \bar{l}(a)\bar{b}F(a) \frac{1 - e^{-(\lambda+\gamma)a}}{\lambda + \gamma} da \frac{f'(\tilde{x})}{f(\tilde{x})} \Delta_x , \quad \text{(A14)}$$

which shows that the braced term in the element s_{22} of the characteristic equation reflects the influence of the growth curve plasticity upon the food intake rate of the *Daphnia* population.

References

1. Bazykin, A. D., Berezovskaya, F. S., Denisov, G. A., Kuznetzov, Yu. A.: The influence of predator saturation effect and competition among predators on predator-prey system dynamics. Ecol. Model. **14**, 39–57 (1981)
2. Beverton, R. J. H., Holt, S. J.: The dynamics of exploited fish populations. London: Her Majesty's Stationary Office 1957
3. De Roos, A. M.: Numerical methods for structured population models: the escalator boxcar train. Num. Meth. Part. Differ. Equations **4**, 173–195 (1988)
4. De Roos, A. M., Diekmann, O., Metz, J. A. J.: The escalator boxcar train: basic theory and an application to *Daphnia* population dynamics. CWI report AM-R8814, Centre for Mathematics and Computer Science, Amsterdam, The Netherlands 1989
5. Huston, M. A., DeAngelis, D. L., Post, W. M.: New computer models unify ecological theory. Bioscience **38**, 682–691 (1989)
6. Jansen, V. A. A., Nisbet, R. M., Gurney, W. S. C.: Generation cycles in stage structured populations. Bull. Math. Biol. (in press)
7. Kooijman, S. A. L. M., Metz, J. A. J.: On the dynamics of chemically stressed populations: The deduction of population consequences from effects on individuals. Ecotox. Env. Saf. **8**, 254–274 (1984)
8. McCauley, E., Murdoch, W. W.: Cyclic and stable populations: plankton as a paradigm. Am. Natur. **129**, 97–121 (1987)
9. Metz, J. A. J., Diekmann, O.: The dynamics of physiologically structured populations. (Lect. Notes Biomath., vol. 68) Berlin Heidelberg New York: Springer 1982

10. Metz, J. A. J., De Roos, A. M., Van den Bosch, F.: Population models incorporating physiological structure: a quick survey of the basic concepts and an application to size-structured population dynamics in waterfleas. In: Ebenman, B., Persson, L. (eds.) Size-structured populations: ecology and evolution. Berlin Heidelberg New York: Springer 1988
11. Murphy, L. F.: A nonlinear growth mechanism in size-structured population dynamics. J. Theor. Biol. **104,** 493–506 (1983)
12. Nisbet, R. M., Gurney, W. S. C.: Modelling fluctuating populations. New York: Wiley 1982
13. Nisbet, R. M., Gurney, W. S. C.: "Stage-structure" models of uniform larval competition. In: Levin, S. A., Hallam, T. G. (eds.) Mathematical ecology. Proceedings Trieste 1982. (Lect. Notes Biomath. vol. 54, pp. 97–113) Berlin Heidelberg New York: Springer 1984
14. Rosenzweig, M. L.: Paradox of enrichment: destabilization of exploitation ecosystems in ecological time. Science (Wash., D.C.) **171,** 385–387 (1971)
15. Sauer, J. R., Slade, N. A.: Size-based demography of vertebrates. Ann. Rev. Ecol. Syst. **18,** 71–90 (1987)
16. Thieme, H. R.: Well-posedness of physiologically structured population models for *Daphnia magna*. J. Math. Biol. **26,** 299–317 (1988)
17. Van den Bosch, F., Metz, J. A. J., Diekmann, O.: The velocity of spatial population expansion. CWI report AM-R8812, Centre for Mathematics and Computer Science, Amsterdam, The Netherlands 1988
18. Werner, E. E., Gilliam, J. F.: The ontogenetic niche and species interactions in size-structured populations. Ann. Rev. Ecol. Syst. **15,** 393–425 (1984)
19. Wollkind, D. J., Collings, J. B., Logan, J. A.: Metastability in a temperature-dependent model system for predator-prey mite outbreak interactions on fruit trees. Bull. Math. Biol. **50,** 379–409 (1988)